Modelling An Experiment To Study Surface Dilation Effects



Keith Gillow
St. Catherine's College
Oxford

Dissertation submitted in partial fulfillment of the requirements
for the degree of Master of Science in
Mathematical Modelling and Numerical Analysis
at the University of Oxford
September 1995

Acknowledgments

I would like to thank Dr Hilary Ockendon for suggesting the topic of this dissertation and for her encouragement and guidance as my supervisor, Dr Richard Darton for answering my questions on the overflowing cylinder and foams in general, Helena Grunnet-Jepsen for providing some of the results of her research and the Engineering and Physical Sciences Research Council for their funding throughout the year. I would also like to thank the late Dr Alan B. Tayler C.B.E. without whose advice I might never have taken this course. Finally I would like to thank my parents for all their faith and interest.

Contents

1 Introduction **1**

1.1 The Overflowing Cylinder Technique 2

1.2 Previous Research 4

1.3 Dissertation Aims 6

2 A 2-Dimensional Model **7**

2.1 Dimensional Model 11

2.2 Non-Dimensionalisation 11

3 An Asymptotic Solution **13**

4 A Combined Analytical And Numerical Solution **17**

5 A 3-Dimensional Model **30**

5.1 Dimensional Model 31

5.2 Non-Dimensionalisation 31

5.3 An Asymptotic Solution 32

6 Surface Tension Gradients **37**

7 Conclusion **40**

A The Numerical Program **41**

Chapter 1

Introduction

It is well known that surface active agents play an important role in the foaming properties of liquids. Experience shows that these properties strongly depend on both the nature and the amount of the applied surfactant. The stability of the created foams against coalescence is, for the greater part, determined by the stability of the thin liquid films in between the air bubbles. In turn, the stability of these thin liquid films largely depends on the interfacial properties of the liquid. However the liquid-air interfaces are continuously exposed to all kinds of disturbances, especially during preparation, storage, and usage when compression and expansion of the interfaces occur. Examination of the dynamic interfacial properties of the liquid may therefore increase our knowledge of the behaviour of foams.

One of the ways in which a mechanical disturbance can be applied to a liquid surface is by means of an expansion or compression of that surface. This expansion or compression can be achieved in several ways. In a so-called dynamic measurement the surface is subjected to a sinusoidal change in surface area. In another type of measurement the surface is continually expanded or compressed. Because a thin liquid film can be made unstable, especially when it is subjected to an expansion, the study of a continually expanding surface can result in a better understanding of the foaming behaviour of a liquid.

In practice expanding surfaces can be found during the preparation of foams, nucleation of bubbles, and during the application of thin liquid layers, such as paints, coatings, printing inks e.t.c., on solid walls. Knowledge of the dynamic interfacial properties of these liquids may lead to the improvement of products and production techniques.

One way to accomplish a pure dilation is with the use of an overflowing cylinder.

1.1 The Overflowing Cylinder Technique

The overflowing cylinder (see Figure 1.1) consists of a cylinder of diameter ten centimetres through which a liquid is pumped upward. In order to ensure a laminar flow field in the cylinder the fluid is first passed through a conical tube having a small slope (1:10) before it reaches the cylinder (a flow straightener may also be included in the cylinder). Next the liquid is allowed to flow over the rim of the vertical cylinder causing a circular liquid surface to be expanded continuously in a radial way. Care must be taken to ensure that the outside of the cylinder wall is completely wetted by the falling film. We are dealing with a steady state situation which means the surface dilation pattern does not change in time. However, when the flow rate is altered a new surface expansion rate will be established. The existence of such a stable steady state is questioned by Schulkes in his paper [9] in which he considers the initial phase of the flow from when the apparatus is first switched on. The paper includes clear photographs of experiments performed as well as a detailed numerical treatment.

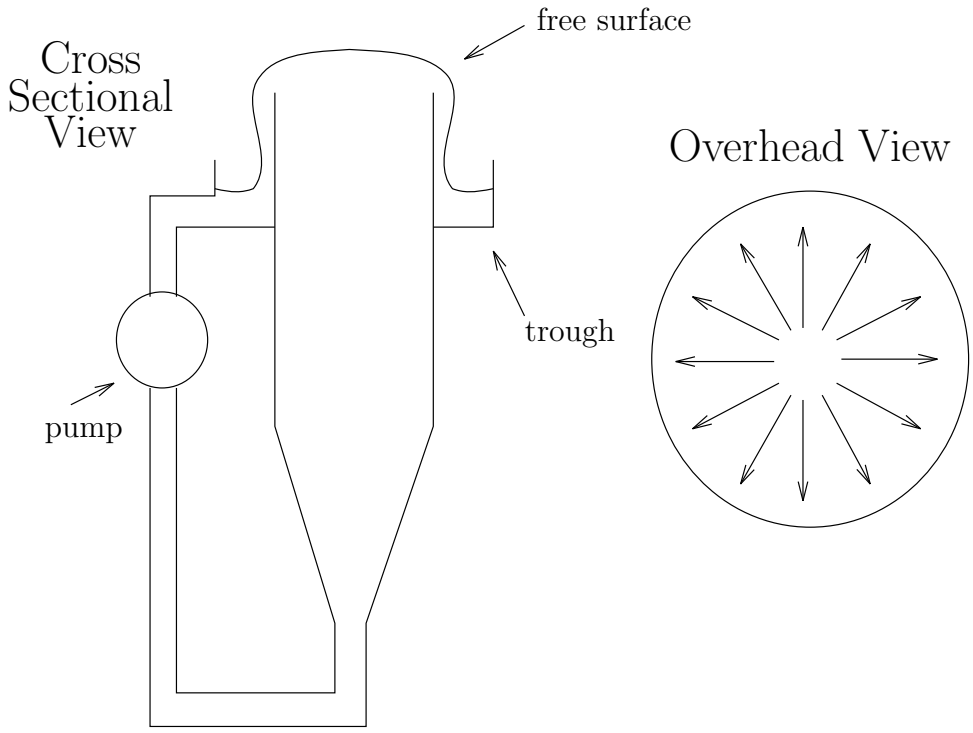


Figure 1.1: The Overflowing Cylinder (not to scale).

Using this apparatus it is possible to measure the radial velocity of the free surface, the shape of the free surface and the surface tension. To measure the surface tension a standard procedure known as the Wilhelmy plate technique is used. Here a platinum plate, or glass rod, attached to a balance is carefully moved downwards by a stepper motor. A sudden increase in weight is seen when the plate touches the surface, followed by a decrease in weight as the plate is further immersed. The plate is then slowly withdrawn and the value of the surface tension is deduced from the excess weight when its lower edge becomes level with the liquid surface. This method ensures that the plate is well wetted so that the contact angle is zero. To measure the radial velocity the surface is sprinkled with fine particles and then photographed from above at fixed time intervals (experimentally it is found that these particles do not influence the equilibrium surface tension of water). By comparing the photographs it is then possible to calculate the velocity of various points on the free surface. Using these results the relative surface expansion rate, as defined below, can be calculated.

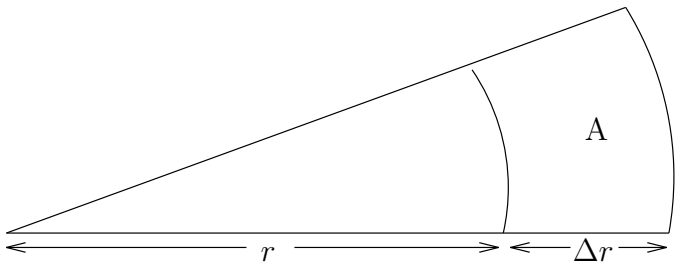


Figure 1.2: Definition of the surface area A.

$$\text{relative surface expansion rate} = \lim_{\Delta r \to 0} \frac{d \ln A}{dt} \tag{1.1}$$

$$= \frac{v_r}{r} + \frac{\partial v_r}{\partial r} \tag{1.2}$$

where the free surface is assumed to be almost flat and v_r is the radial component of the velocity at the surface.

A key question of interest to those experimenting with this apparatus is how to relate the relative surface expansion rate to the flow rate through the funnel of the overflowing cylinder. This problem appears to be a difficult one and to my knowledge none of the investigations previously done have resulted in a detailed description of the physical mechanism which explains the operation of the overflowing cylinder technique.

1.2 Previous Research

The problem of the overflowing cylinder has been previously studied by several people. One of the most recent studies was by Bergink-Martens et al [1], [2]. In [1] they present the results of a numerical solution in the case of an inviscid fluid with zero and constant surface tension, as well as some results obtained from experiments conducted. A summary of these numerical and experimental results can be seen in figures 1.3 ,1.4 and 1.5.

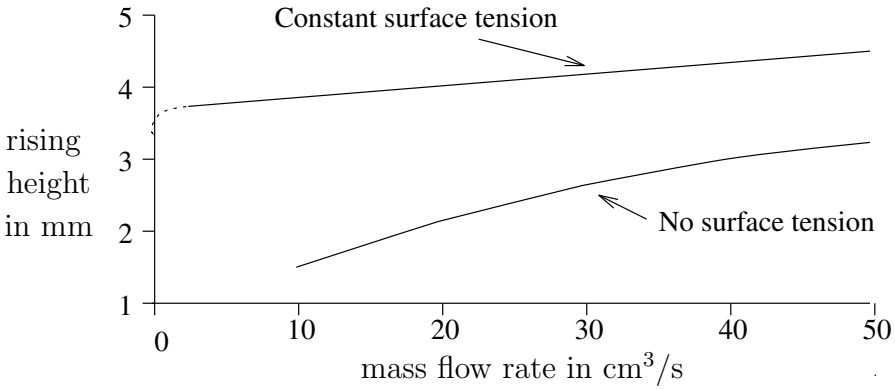


Figure 1.3: The rising height of the interface above the rim of the cylinder as a function of the mass flow rate through the cylinder (numerical results).

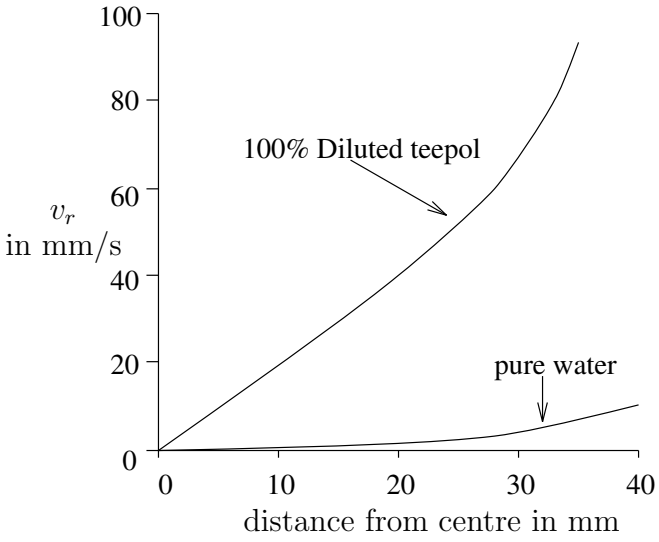


Figure 1.4: The velocity of the surface as a function of the radius at a flow rate of 7.6cm^3/s (experimental results).

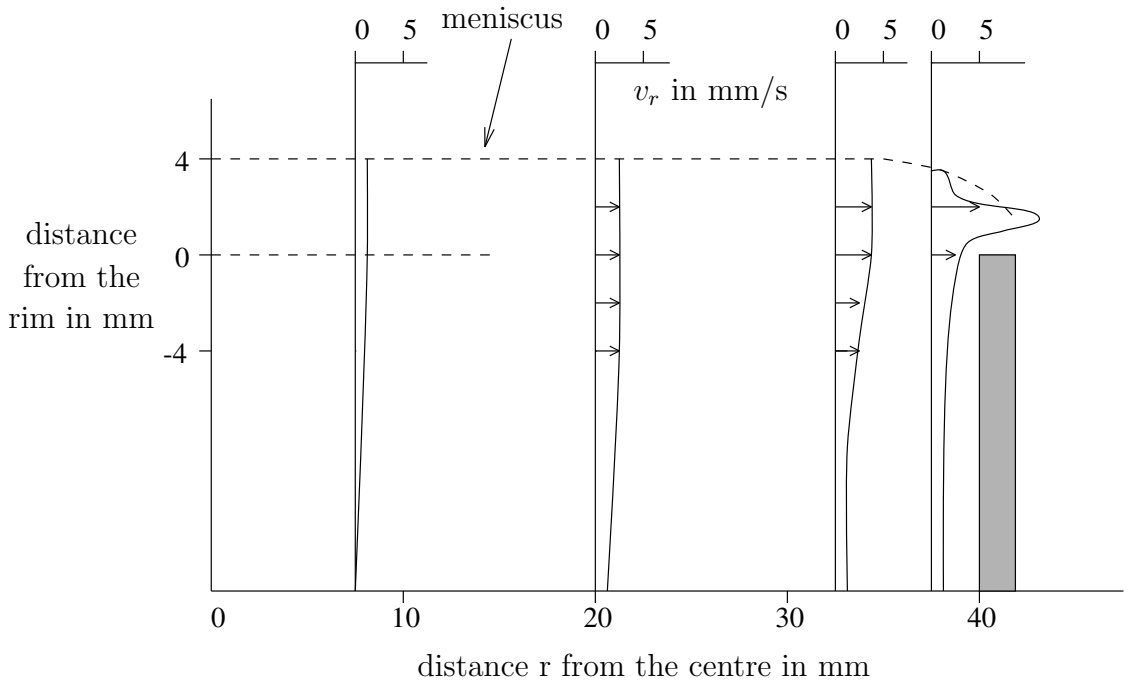


Figure 1.5: The velocity distribution in pure water at a flow rate of 7.6cm^3/s and a constant surface tension (numerical results).

From these results Bergink-Martens et al concluded that in the case of an inviscid fluid flowing through the overflowing cylinder, a better than quantitative agreement exists between their calculations and measurements. The calculated results show that in the neighbourhood of the rim the bulk fluid is driving the surface layer. That is the maximum radial velocity in the fluid at a small horizontal distance from the rim occurs below the fluid surface. If a small amount of surfactant is added the surface tension is decreased and surface tension gradients are introduced, resulting in a large change in magnitude of the surface velocity. They conclude this suggests that in this case the maximum radial velocity indeed occurs at the surface, and the surface is driving the bulk.

In [2] they consider in more detail the effect of these surface tension gradients. They present experimental results showing how the surface tension varies across the surface and how it is effected by changes in the concentration of the surfactant used. They give details of how they have tried to model the surface as a thin layer which behaves differently to the bulk flow but matches with it where they meet. The resulting model gives predictions of the relationship between the surface tension and

the distance from the axis of symmetry which although they do not agree with the experimental results are of the the same order.

Similar experiments have recently been conducted at the Department of Engineering Sciences, University of Oxford, by Grunnet-Jepsen as part of her Doctorate research program. Some of the results of this research can be seen in [4], but for a detailed account and conclusions we must wait for the publication of a completed Thesis. In their experiments they have experimented with different flow rates and surfactant concentrations in order to produce results which show the most marked changes from those obtained when using pure water. Clearly the flow rate can only be increased so far before the falling film leaves the side of the cylinder. At very low flow rates, on the other hand, instabilities occur probably caused by the thin film entering the pool of fluid in the trough.

1.3 Dissertation Aims

In this dissertation I shall begin by looking at the simpler problem of inviscid flow through a two dimensional nozzle. With the use of some basic assumptions I shall describe a possible model for the flow. In chapter 3 I shall consider the possibility of an analytical solution whilst in chapter 4 I shall describe and give some results of a combined analytical and numerical approach. The analysis in both these chapters will be restricted to the case of constant surface tension as surface tension gradients cannot occur in the case of an inviscid fluid as will be proved in the derivation of the model used. Following this I shall construct a similar model for the three dimensional case and as in chapter 3 I shall show how an asymptotic outer solution may be obtained. This solution will then be compared, in a particular case, with some experimental results. In chapter 6 I shall discuss how a variable surface tension might be modelled. Finally I shall conclude and indicating possible areas that need further consideration. [1]

[1] Much of the background information in this chapter was taken from [1].

Chapter 2

A 2-Dimensional Model

Since the cylinder is much longer than it is wide the effects of the flow into the trough will be neglected. Thus in two dimensions a suitable diagram of the problem is shown in figure 2.1 below.

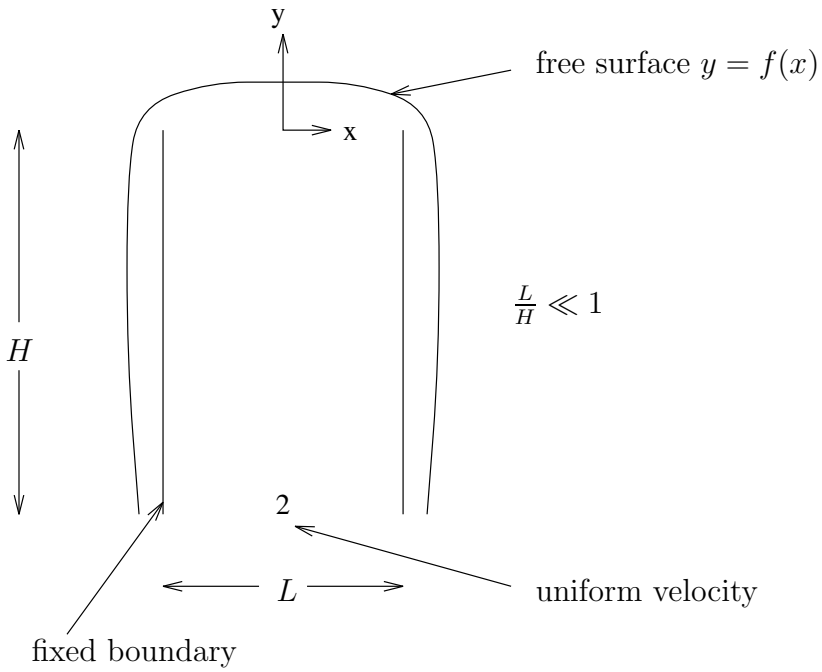


Figure 2.1: A diagram of the 2-dimensional model.

At 2 the flow will be almost uniform. Taking the flow there to be exactly uniform means it is also irrotational at 2. Now provided all the streamlines of the flow emanate from 2 then the entire flow must be irrotational. The possibility of any closed streamlines in the flow leading to rotationality seems unlikely. Since the fluid is a liquid it will be almost incompressible. As was stated in the introduction we shall

begin by restricting ourselves to an inviscid fluid and we expect the flow to be steady. We therefore have so far the four basic assumptions that the flow is :-

- incompressible
- irrotational
- inviscid
- steady

From these we have the following three equations :-

$$\nabla.\mathbf{u} = 0 \qquad \text{in fluid} \tag{2.1}$$

$$\nabla \times \mathbf{u} = 0 \qquad \text{in fluid} \tag{2.2}$$

$$(\mathbf{u}.\nabla)\mathbf{u} = -\frac{1}{\rho}\nabla p + \mathbf{g} \qquad \text{in fluid} \tag{2.3}$$

where

- $\mathbf{u} = (u, v)$ is the velocity of the fluid,
- p is the pressure in the fluid,
- ρ is the density of the fluid (constant) and
- $\mathbf{g}$ is the acceleration due to gravity.

Equation (2.2) implies there exist a ϕ such that $\mathbf{u} = \nabla\phi$ which on substitution into (2.1) and (2.3) leads to :-

$$\nabla^2\phi = 0 \qquad \text{in fluid} \tag{2.4}$$

$$\frac{1}{2}|\nabla\phi|^2 + \frac{p}{\rho} + gy = C \qquad \text{in fluid} \tag{2.5}$$

where C is a constant.

At the fixed boundaries we have the condition :-

$$u = 0 \qquad \text{on} \quad x = \pm\frac{1}{2}L \ , \ -H < y < 0 \tag{2.6}$$

$$\Rightarrow \ \phi_x = 0 \qquad \text{on} \quad x = \pm\frac{1}{2}L \ , \ -H < y < 0 \tag{2.7}$$

At the free surface we need two conditions :-

i) **u** is tangent to the surface

$$\Rightarrow \quad v \;=\; uf' \qquad \text{on} \quad y = f(x) \tag{2.8}$$

$$\Rightarrow \quad \phi_y \;=\; \phi_x f' \qquad \text{on} \quad y = f(x) \tag{2.9}$$

ii) Consider a small element of surface as shown below :-

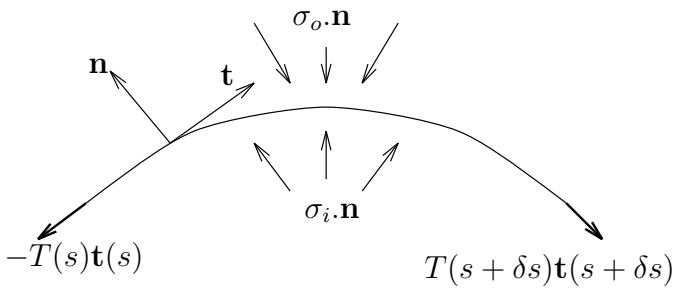


Figure 2.2: The forces on a section of the free surface.

where

- s is arc length,
- $\mathbf{t}$ is a unit tangent vector,
- $\mathbf{n}$ is a unit normal vector,
- T is the surface tension force,
- σ is the stress tensor,
- $\sigma_o.\mathbf{n}$ is the stress acting on the outside of the surface and
- $\sigma_i.\mathbf{n}$ is the stress acting on the inside of the surface.

A simple force balance hence gives :-

$$T(s+\delta s)\mathbf{t}(s+\delta s) - T(s)\mathbf{t}(s) + \int_s^{s+\delta s} (\sigma_o - \sigma_i).\mathbf{n}\, ds \;=\; 0 \tag{2.10}$$

Using a Taylor expansion of the first term gives :-

$$[T(s) + T'(s)\delta s]\,[\mathbf{t}(s) + \mathbf{t}'(s)\delta s] - T(s)\mathbf{t}(s) + \int_s^{s+\delta s} (\sigma_o - \sigma_i).\mathbf{n}\, ds + O((\delta s)^2) = 0$$

$$\Rightarrow \quad T(s)\mathbf{t}'(s) + T'(s)\mathbf{t}(s) + \frac{1}{\delta s}\int_s^{s+\delta s} (\sigma_o - \sigma_i).\mathbf{n}\, ds + O(\delta s) \quad = \quad 0 \qquad (2.11)$$

Therefore taking the limit as $\delta s \to 0$ gives :-

$$T\mathbf{t}' + T'\mathbf{t} + (\sigma_o - \sigma_i).\mathbf{n} \quad = \quad 0 \qquad \text{on} \quad y = f(x) \qquad (2.12)$$

Using the Serret Frenet formula $\mathbf{t}' = \kappa\mathbf{n}$ (where κ is the curvature) gives :-

$$T\kappa\mathbf{n} + T'\mathbf{t} + (\sigma_o - \sigma_i).\mathbf{n} \quad = \quad 0 \qquad \text{on} \quad y = f(x) \qquad (2.13)$$

Now for an inviscid fluid $\sigma = -p\delta_{ij}$. Hence :-

$$(T\kappa + p - p_o)\mathbf{n} \quad = \quad -T'\mathbf{t} \qquad \text{on} \quad y = f(x) \qquad (2.14)$$

But $\mathbf{n}$ is perpendicular to $\mathbf{t}$. Thus :-

$$p \quad = \quad p_o - T\kappa \qquad \text{on} \quad y = f(x) \qquad (2.15)$$

$$T' \quad = \quad 0 \qquad \text{on} \quad y = f(x) \qquad (2.16)$$

Equation (2.16) therefore implies T remains constant along the free surface. If we had taken the more complex case of a viscous fluid then the possibility of shear forces would have meant that surface tension gradients were possible. Combining (2.5) evaluated at the free surface and (2.15) gives :-

$$\frac{1}{2}|\nabla\phi|^2 + \frac{p_o}{\rho} - \frac{T\kappa}{\rho} + gy \quad = \quad C \qquad \text{on} \quad y = f(x) \qquad (2.17)$$

Finally noting $\kappa = \frac{f''}{(1+f'^2)^{\frac{3}{2}}}$ and absorbing the term $\frac{p_o}{\rho}$ into C gives :-

$$\frac{1}{2}|\nabla\phi|^2 - \frac{Ty''}{\rho(1+y'^2)^{\frac{3}{2}}} + gy \quad = \quad C \qquad \text{on} \quad y = f(x) \qquad (2.18)$$

as the second condition on the free surface.

Assuming the flow is uniform as it enters the channel implies :-

$$u = 0 \ , \ v = U \qquad \text{on} \quad y = -H \ , \ |x| \leq \frac{1}{2}L \qquad (2.19)$$

$$\Rightarrow \quad \phi_x = 0 \ , \ \phi_y = U \qquad \text{on} \quad y = -H \ , \ |x| \leq \frac{1}{2}L \qquad (2.20)$$

We now have left only the need for a condition on the falling film in order to give boundary conditions on a closed curve. The falling film should have a jet like behaviour. That is, we assume that at $y = -K$ ($\frac{L}{K} \ll 1$) the vertical component of

velocity, v, has the same value for all points x in the falling film whilst the horizontal velocity component, u, is zero. Also as $K \to \infty$, $v \to -\infty$. Thus :-

$$u = 0 \ , \ v = -V \qquad \text{on} \quad y = -K \ , \ \frac{1}{2}L \leq |x| \leq X \tag{2.21}$$

$$\Rightarrow \ \ \phi_x = 0 \ , \ \phi_y = -V \qquad \text{on} \quad y = -K \ , \ \frac{1}{2}L \leq |x| \leq X \tag{2.22}$$

where $X = f^{-1}(-K)$. Since mass flux must always be conserved we then have :-

$$UL = V|2X - L| \tag{2.23}$$

Thus we now have a complete set of equations governing the velocity of the fluid and the position of the free boundary. Namely (2.4), (2.7), (2.9), (2.18), (2.20), (2.22) and (2.23).

2.1 Dimensional Model

The equations listed above are included here together for clarity and ease of reference.

$$\nabla^2\phi = 0 \qquad \text{in fluid} \tag{2.24}$$

$$\phi_x = 0 \qquad \text{on} \quad x = \pm\frac{1}{2}L \ , \ -H < y < 0 \tag{2.25}$$

$$\phi_y = \phi_x f' \qquad \text{on} \quad y = f(x) \tag{2.26}$$

$$\frac{1}{2}|\nabla\phi|^2 - \frac{Tf''}{\rho(1+f'^2)^{\frac{3}{2}}} + gy = C \qquad \text{on} \quad y = f(x) \tag{2.27}$$

$$\phi_x = 0 \qquad \text{on} \quad y = -H \ , \ |x| \leq \frac{1}{2}L \tag{2.28}$$

$$\phi_y = U \qquad \text{on} \quad y = -H \ , \ |x| \leq \frac{1}{2}L \tag{2.29}$$

$$\phi_x = 0 \qquad \text{on} \quad y = -K \ , \ \frac{1}{2}L \leq |x| \leq X \tag{2.30}$$

$$\phi_y = -\frac{UL}{|2X - L|} \quad \text{on} \quad y = -K \ , \ \frac{1}{2}L \leq |x| \leq X \tag{2.31}$$

2.2 Non-Dimensionalisation

Taking U as a typical velocity scale and L as a typical length scale a suitable non-dimensionalisation is :-

$$\mathbf{u} = U\tilde{\mathbf{u}} \quad , \quad \mathbf{x} = L\tilde{\mathbf{x}} \quad , \quad f = L\tilde{f} \quad , \quad \phi = UL\tilde{\phi} \quad , \quad X = L\tilde{X}$$

which on substituting into the above model and dropping the tildes gives the following set of non-dimensional equations.

$$\nabla^2\phi = 0 \qquad \text{in fluid} \tag{2.32}$$

$$\phi_x = 0 \qquad \text{on} \quad x = \pm\frac{1}{2} \ , \ -M_1 < y < 0 \tag{2.33}$$

$$\phi_y = \phi_x f' \qquad \text{on} \quad y = f(x) \tag{2.34}$$

$$\frac{1}{2}|\nabla\phi|^2 + \frac{y}{F^2} - \frac{Gf''}{(1+f'^2)^{\frac{3}{2}}} = C \qquad \text{on} \quad y = f(x) \tag{2.35}$$

$$\phi_x = 0 \qquad \text{on} \quad y = -M_1 \ , \ |x| \leq \frac{1}{2} \tag{2.36}$$

$$\phi_y = 1 \qquad \text{on} \quad y = -M_1 \ , \ |x| \leq \frac{1}{2} \tag{2.37}$$

$$\phi_x = 0 \qquad \text{on} \quad y = -M_2 \ , \ \frac{1}{2} \leq |x| \leq X \tag{2.38}$$

$$\phi_y = -\frac{1}{|2X-1|} \quad \text{on} \quad y = -M_2 \ , \ \frac{1}{2} \leq |x| \leq X \tag{2.39}$$

where

$$F^2 = \frac{U^2}{gL} \quad , \quad G = \frac{T}{\rho L U^2} \quad , \quad M_1 = \frac{H}{L} \quad , \quad M_2 = \frac{K}{L}$$

Now that we have a well defined non-dimensional model we are in a position to attempt to find some solutions.

Chapter 3

An Asymptotic Solution

The range of flow rates used experimentally and the magnitude of the surface tension measured are small and hence the parameters F and G are found to be small (typically F is $O(10^{-2})$ and G is $O(10^{-1})$ or $O(1)$). Recalling equation (2.35) we have :-

$$\frac{F^2}{2}|\nabla\phi|^2 + f - F^2 G\frac{f''}{(1+f'^2)^{\frac{3}{2}}} \;=\; F^2 C \qquad \text{on} \quad y = f(x) \tag{3.1}$$

Assuming ϕ_x, ϕ_y, f' and f'' are $O(1)$ then since $F^2G \ll F^2C \ll 1$ and $F^2 \ll F^2C \ll 1$ balancing the dominant terms gives :-

$$f \;=\; F^2 C \;\ll\; 1 \tag{3.2}$$

Therefore to $O(1)$ the free surface is $f = 0$.

To simplify the modelling of the falling film a good first approximation (at least as far as the flow within the cylinder is concerned) would be to model the two points on the rim as sinks. That is :-

$$\phi(x,y) \;\sim\; -\frac{1}{2\pi}\ln\left(\left(x \pm \frac{1}{2}\right)^2 + y^2\right) \qquad \text{near} \quad x = \mp\frac{1}{2}\ ,\ y = 0 \tag{3.3}$$

Since $M_1 \gg 1$ we shall assume the channel is infinitely long in the negative y direction.

With these assumptions to $O(1)$ the non-dimensional model and diagram are :-

$$\nabla^2\phi \;=\; 0 \qquad \text{in fluid} \tag{3.4}$$

$$\phi_x \;=\; 0 \qquad \text{on} \quad x = \pm\frac{1}{2}\ ,\ y < 0 \tag{3.5}$$

$$\phi_y \;=\; 0 \qquad \text{on} \quad |x| \le \frac{1}{2}\ ,\ y = 0 \tag{3.6}$$

$$\phi_x \;\to\; 0 \qquad \text{as} \quad y \to -\infty\ ,\ |x| \le \frac{1}{2} \tag{3.7}$$

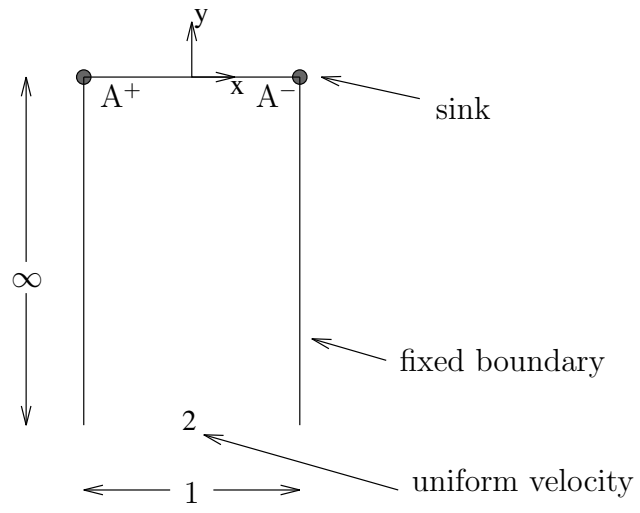


Figure 3.1: A diagram of the simplified 2-dimensional model.

$$\phi_y \rightarrow 1 \qquad \text{as} \quad y \rightarrow -\infty \ , \ |x| \leq \frac{1}{2} \tag{3.8}$$

$$\phi(x,y) \sim -\frac{1}{2\pi} \ln\left(\left(x \pm \frac{1}{2}\right)^2 + y^2\right) \qquad \text{near } \mathrm{A}^{\pm} \tag{3.9}$$

Now the conformal mapping $\zeta = \sin(\pi z)$, where $z = x + iy$, maps the semi infinite strip to the lower half of the ζ plane. The images of the sinks are $(-1, 0)$ and $(1, 0)$. Thus the complex potential $w = \phi + i\psi$, where ψ is a stream function, can be written as :-

$$w(z) = -\frac{1}{2\pi}(\ln(\zeta - 1) + \ln(\zeta + 1)) \tag{3.10}$$

Therefore :-

$$u - iv = \frac{dw}{dz} \tag{3.11}$$

$$= \frac{dw}{d\zeta}\frac{d\zeta}{dz} \tag{3.12}$$

$$= -\frac{\zeta}{\zeta^2 - 1}\cos(\pi z) \tag{3.13}$$

$$= \tan(\pi z) \tag{3.14}$$

Equating real and imaginary parts gives :-

$$\phi_x = \frac{\sin(\pi x)\cos(\pi x)}{\cos^2(\pi x)\cosh^2(\pi y) + \sin^2(\pi x)\sinh^2(\pi y)} \tag{3.15}$$

$$\phi_y = \frac{-\sinh(\pi y)\cosh(\pi y)}{\cos^2(\pi x)\cosh^2(\pi y) + \sin^2(\pi x)\sinh^2(\pi y)} \tag{3.16}$$

Plots of these two functions can be seen on below. From these it is clear to see that the original assumption that ϕ_x and ϕ_y remain $O(1)$ fails near the corners.

The above approximation breaks down as the sinks are approached when the appropriate length scales are much smaller and the velocity scales much larger than was assumed in our initial scaling. Thus we need to consider an inner problem near $x = \frac{1}{2}L$, $y = 0$. The inner problem is essentially that of a pouring flow which has been studied numerically by Vanden-Broeck and Keller [10]. The resultant solution gives rise to a free surface shape which tends to a constant as the distance from the lip increases. Thus matching the outer and inner solutions will determine the value of the constant C in the outer solution.

It turns out that to solve this inner problem is no more difficult than solving the full 2-dimensional problem using a combined analytical and numerical method based on Dias and Vanden-Broeck [5] which is described in chapter 4.

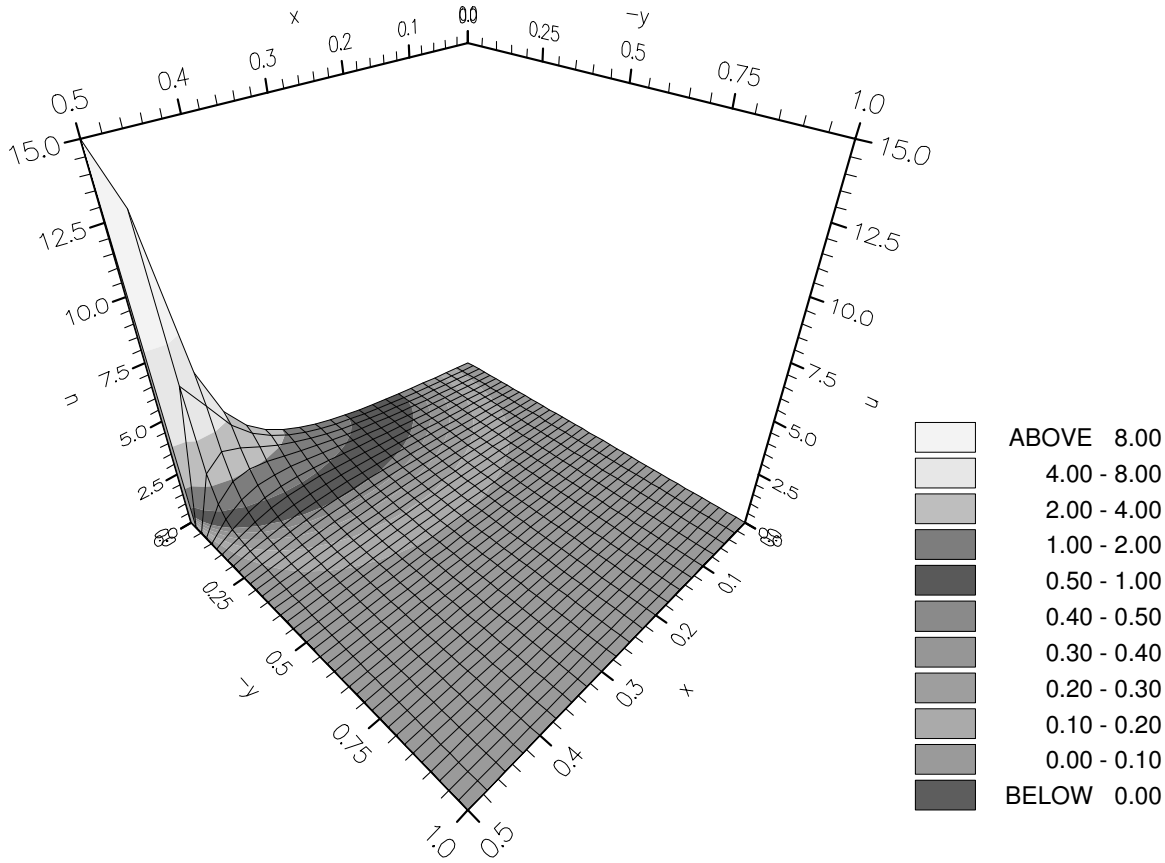


Figure 3.2: Graph of the outer solution for u.

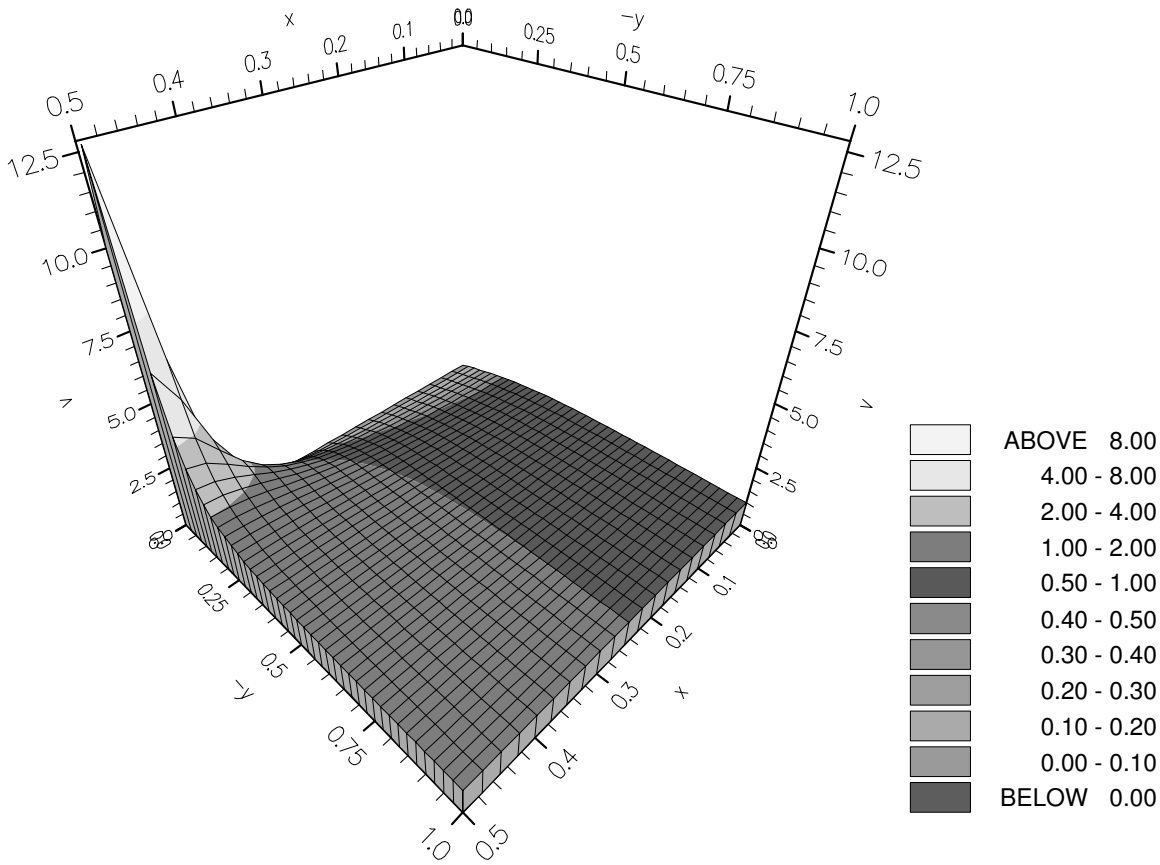


Figure 3.3: Graph of the outer solution for v.

Chapter 4

A Combined Analytical And Numerical Solution

As in the previous chapter we shall assume the nozzle is infinitely long. We take as our diagram of the flow figure 4.1 where the key points of the flow have each been labelled. As stated in the previous chapter we shall use a technique based upon that of Dias and Vanden-Broeck [5] who studied the problem of flow through a nozzle inclined to the vertical without including any surface tension effects. By introducing a complex potential and using a conformal map we will first transform the infinite open flow domain to a finite closed flow domain. Combining the asymptotic forms of the hodograph variable at the key points it is possible to construct a hodograph variable,

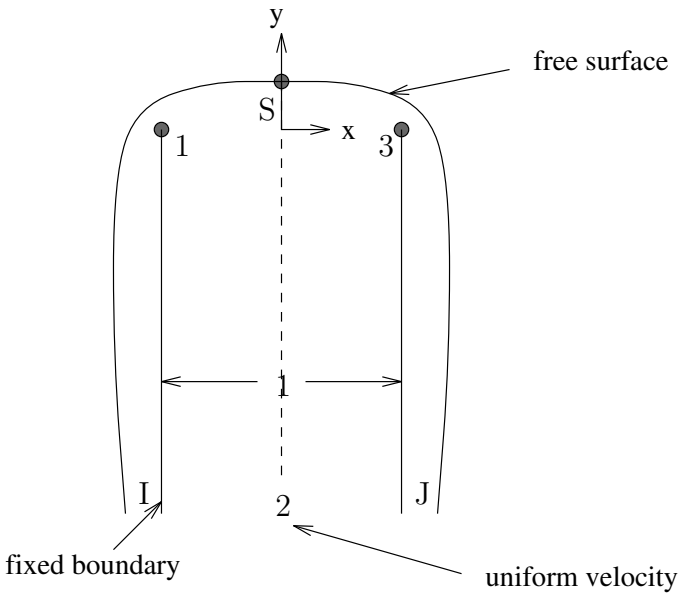


Figure 4.1: A diagram of the 2-dimensional model with key points labelled.

containing a power series with unknown coefficients, which satisfies all the boundary conditions except for Bernoulli's equation at the free surface. Using this condition and a technique known as collocation we determine the unknown coefficients which gives us a formula for the velocity at every point in the flow. Finally using numerical integration we find the position of the free surface relative to the rim of the nozzle.

We shall define a stream function ψ by the pair of equations :-

$$\psi_x = -\phi_y \tag{4.1}$$

$$\psi_y = \phi_x \tag{4.2}$$

At 2 we again assume the flow will be uniform. Thus :-

$$\phi \sim y + B \qquad \text{at 2} \tag{4.3}$$

$$\Rightarrow \ \psi \sim -x + C \qquad \text{at 2} \tag{4.4}$$

where B and C are constants. Since by definition the stream function ψ satisfies $(\mathbf{u}.\nabla)\psi = 0$ it remains constant along any given streamline. Now the fixed and free boundaries must form two streamlines. The free boundary streamline also includes the line of symmetry of the flow. Since we know the form of ψ at 2 and choosing $\phi = 0 = \psi$ at S we have :-

$$\psi = \frac{1}{2} \qquad \text{on } 2_a 1 \mathrm{I}_a \tag{4.5}$$

$$\psi = -\frac{1}{2} \qquad \text{on } 2_b 3 \mathrm{J}_a \tag{4.6}$$

$$\psi = 0 \qquad \text{on } \mathrm{J}_b \mathrm{S} 2 \mathrm{S} \mathrm{I}_b \tag{4.7}$$

Also at 2 $\phi \sim -\infty$ whilst at I and J $\phi \sim \infty$. Hence the flow domain in the f plane, where $f = \phi + i\psi$ is the complex potential, is :-

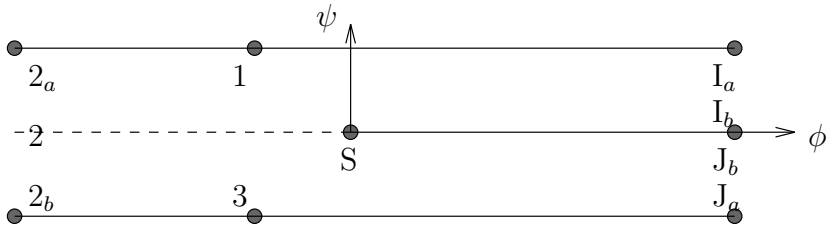


Figure 4.2: The flow domain in the f plane.

Now using the Schwartz Christoffel theorem we find that the conformal mapping :-

$$f = \frac{1}{\pi} \ln \left(\frac{s}{(s^2-1)^{\frac{1}{2}}} \right) \tag{4.8}$$

maps the f plane into the upper half of the s plane as shown in figure 4.3. Then using the map :-

$$r = \sqrt{\left(\frac{s-1}{s+1} \right)} \tag{4.9}$$

maps the s plane into the first quadrant of the r plane as shown in figure 4.4. Finally using the mapping :-

$$t = \frac{i-r}{i+r} \tag{4.10}$$

maps the r plane into the closed half disc of radius 1 in the t plane as shown in figure 4.5.

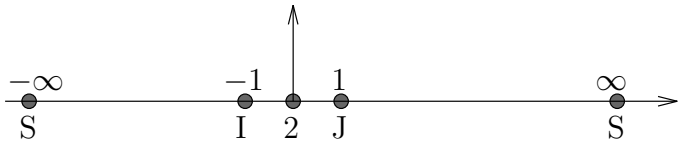


Figure 4.3: The flow domain in the s plane.



Figure 4.4: The flow domain in the r plane.

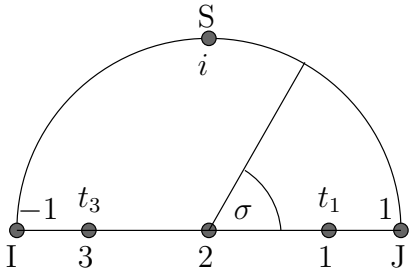


Figure 4.5: The flow domain in the t plane.

Combining these maps we have :-

$$f \;=\; \frac{1}{\pi}\ln\left(\frac{2it}{(t^2-1)}\right) \tag{4.11}$$

which maps the open infinite flow domain in the f plane to the closed finite flow domain in the t plane. Note that the fixed boundary has been mapped to the diameter of the semi-circle while the free boundary has been mapped to the semi-circular arc.

Defining the angle σ as shown in figure 4.5 we see that points on the free boundary have, in the t plane, positions $t = e^{i\sigma}$ for $\sigma \in (0, \pi)$. As before Bernoulli's equation :-

$$\frac{1}{2}(u^2+v^2) + \frac{1}{F^2}y - G\kappa \;=\; C \tag{4.12}$$

is satisfied on the free surface. Introducing the Hodograph variable $\zeta = \frac{df}{dz} = u - iv$ the problem is to find ζ as an analytic function of t satisfying (4.12), the kinematic conditions and having the appropriate singularities. The kinematic conditions being that the flow is tangential to the fixed and free boundaries.

$\zeta(t)$ must clearly be purely imaginary on the real axis and continuous on the boundary of the half disc except at $t = \pm 1$, $t = t_1$ and $t = t_3$ where it becomes infinite. Hence by the Schwartz reflection principle $\zeta(t)$ can be expanded in a power series convergent in the unit circle $|t| < 1$.

At the point S where the flow separates, the velocity vanishes and the appropriate behaviour for ζ is :-

$$\zeta \;\sim\; t - i \qquad \text{as} \quad t \to i \tag{4.13}$$

By reflection symmetry ζ also has a simple zero at $t = -i$ and no others in $|t| \leq 1$, assuming $t = i$ is the only stagnation point of the flow. Therefore since :-

$$\lim_{t\to i}\frac{\zeta}{1+t^2} \;=\; \frac{1}{2\pi z'} \;\neq\; 0 \tag{4.14}$$

a theorem of Lewy [7] shows that ζ is, moreover, analytic in $|t| \leq 1$ except at $t = \pm 1$, $t = t_1$ and $t = t_3$ and (possibly) $t = \pm i$.

To determine the singularities at I and J we must consider the asymptotic form of a jet falling under gravity. Far along the jet we can write Bernoulli's equation as :-

$$|\zeta^2| \;\sim\; -2F^{-2}y \tag{4.15}$$

having neglected the comparably small terms C and $G\kappa$. Defining the asymptotic jet width to be $\eta(y)$ a flow balance implies $\eta(y)\overline{v}(y) = \frac{1}{2}$, where $\overline{v}$ denotes the average value of v. Using (4.15) we find $\overline{v} \sim (-2F^{-2}y)^{\frac{1}{2}}$ and hence :-

$$\eta(y) \sim \frac{F}{(-8y)^{\frac{1}{2}}} \tag{4.16}$$

Taking a trial guess of $\zeta = (2F^{-2}z)^{\frac{1}{2}}$ gives on a point in the jet $z = \pm\left(\frac{1}{2} + a\eta\right) + iy$ (where $a \in [0,1]$) :-

$$|\zeta^2| = 2F^{-2}\left[\left(\frac{1}{2} + a\eta\right)^2 + y^2\right]^{\frac{1}{2}} \tag{4.17}$$

$$= -2F^{-2}y + O\left(\frac{1}{y^2}\right) \tag{4.18}$$

Thus it satisfies (4.15) to a good approximation. Now :-

$$f - f_1 = \int \zeta\, dz \sim \frac{\sqrt{8}}{3F} z^{\frac{3}{2}} \tag{4.19}$$

where f_1 corresponds monotonely to arc length from S to a given depth. Solving for z and using (4.11) we get to a first approximation :-

$$z \sim \left(\frac{3Ff}{\sqrt{8}}\right)^{\frac{2}{3}} \sim \left[-\frac{3F}{\sqrt{8}\pi}\ln(1 \mp t)\right]^{\frac{2}{3}} \tag{4.20}$$

and

$$\zeta \sim (2F^{-2}z)^{\frac{1}{2}} \sim \left[-\frac{3}{\pi F^2}\ln(1 \mp t)\right]^{\frac{1}{3}} \tag{4.21}$$

If we had gone to a higher order approximation the unknown f_1 would have also been involved (for details see [3]). These singularities at I and J can be combined as :-

$$\zeta \sim [-\ln(1 - t^2)]^{\frac{1}{3}} \qquad \text{as} \quad t \to \pm 1 \tag{4.22}$$

At both extremities of the nozzle, points 1 and 3, the velocity of the fluid is infinite and ζ must have singularities at these points. It is well known that in the case of a flow around the exterior of a corner (at the origin) with an angle α, $f \sim z^{\frac{\pi}{\alpha}}$ (for details see [6]). Now the angle at 1 and 3 is 2π and thus $f \sim \left(z \pm \frac{1}{2}\right)^{\frac{1}{2}}$. Therefore $\zeta \sim \left(z \pm \frac{1}{2}\right)^{-\frac{1}{2}} = f^{-1}$. Thus the appropriate singularities near 1 and 3 are :-

$$\zeta \sim (t - t_1)^{-1} \qquad \text{as} \quad t \to t_1 \tag{4.23}$$

$$\zeta \sim (t - t_3)^{-1} \qquad \text{as} \quad t \to t_3 \tag{4.24}$$

Therefore let :-

$$\zeta(t) = -i(1+t^2)\left(\frac{1-tt_3}{t-t_3}\right)\left(\frac{1-tt_1}{t-t_1}\right)\frac{[-\ln c(1-t^2)]^{\frac{1}{3}}}{[-\ln c]^{\frac{1}{3}}}t_1t_3e^{\Omega(t)} \quad (4.25)$$

c is a constant chosen such that $-\ln c(1-t^2)$ is positive and non zero for $t \in (-1,1)$ (the choice of c does not affect the results, a value $c = 0.2$ will be used in the proceeding calculations). The function $\Omega(t)$ is a Levi-Civita function which is analytic for $|t| < 1$ and continuous for $|t| \leq 1$. It can be expanded in a power series :-

$$\Omega(t) = \sum_{n=1}^{\infty} a_n t^n \qquad a_n \in \Re \quad (4.26)$$

The form (4.25) for ζ has all the appropriate singularites as stated above and satisfies the kinematic conditions for any choice of $\Omega(t)$. Also $\zeta(0) = -i$ which ensures the flow is uniform at 2.

Now using (4.12) and (4.25) we can construct a means of calculating the a_n's and hence completely determine ζ. On $t = e^{i\sigma}$, $\psi = 0$ and hence $f = \phi$. Therefore on the free surface :-

$$\phi(e^{i\sigma}) = \frac{1}{\pi}\ln\left(\frac{2it}{t^2-1}\right)\Big|_{t=e^{i\sigma}} \quad (4.27)$$

$$\Rightarrow \quad \phi(e^{i\sigma}) = \frac{1}{\pi}\ln(\operatorname{cosec}\sigma) \quad (4.28)$$

and $\zeta = \frac{df}{dz} = \frac{d\phi}{dz}$. Therefore :-

$$\frac{dz}{d\phi} = \frac{1}{\zeta} \quad (4.29)$$

$$\Rightarrow \quad \frac{dx}{d\phi} + i\frac{dy}{d\phi} = \frac{u+iv}{u^2+v^2} \quad (4.30)$$

Hence equating real and imaginary parts gives :-

$$\frac{dx}{d\phi} = \frac{u}{u^2+v^2} \quad (4.31)$$

$$\frac{dy}{d\phi} = \frac{v}{u^2+v^2} \quad (4.32)$$

Now using the chain rule :-

$$\frac{dx}{d\sigma} = \frac{dx}{d\phi}\frac{d\phi}{d\sigma} \quad (4.33)$$

$$= -\left(\frac{u}{u^2+v^2}\right)\left(\frac{1}{\pi}\right)\cot\sigma \quad (4.34)$$

and similarly :-

$$\frac{dy}{d\sigma} = -\left(\frac{v}{u^2+v^2}\right)\left(\frac{1}{\pi}\right)\cot\sigma \tag{4.35}$$

Since the equation of free surface has been parameterized in terms of σ, the curvature κ takes the form :-

$$\kappa = \frac{y_\sigma x_{\sigma\sigma} - x_\sigma y_{\sigma\sigma}}{(x_\sigma^2 + y_\sigma^2)^{\frac{3}{2}}} \tag{4.36}$$

which on substituting in from (4.34) and (4.35) becomes :-

$$\kappa = \pi\left(\frac{vu_\sigma - uv_\sigma}{(u^2+v^2)^{\frac{1}{2}}}\right)|\tan\sigma| \tag{4.37}$$

Now differentiating (4.12) with respect to σ gives :-

$$uu_\sigma + vv_\sigma + \frac{1}{F^2}y_\sigma - G\kappa_\sigma = 0 \tag{4.38}$$

which on substituting for y_σ and κ_σ becomes :-

$$\begin{aligned} uu_\sigma + vv_\sigma - \frac{1}{\pi F^2}\left(\frac{v}{u^2+v^2}\right)\cot\sigma + \pi G\Bigg[\frac{(uv_{\sigma\sigma} - vu_{\sigma\sigma})}{(u^2+v^2)^{\frac{1}{2}}}\tan\sigma \\ -\frac{(uv_\sigma - vu_\sigma)(uu_\sigma + vv_\sigma)}{(u^2+v^2)^{\frac{3}{2}}}\tan\sigma + \frac{(uv_\sigma - vu_\sigma)}{(u^2+v^2)^{\frac{1}{2}}}\sec^2\sigma\Bigg]\mathrm{sgn}(\tan\sigma) = 0 \end{aligned} \tag{4.39}$$

To find the forms of u and v on the free boundary we substitute $t = e^{i\sigma}$ into (4.25) and equate real and imaginary parts. By the symmetry of the model it is clear that $t_3 = -t_1$. After some manipulation we find :-

$$u = -M_1 sinA_1 \tag{4.40}$$

$$v = -M_1 cosA_1 \tag{4.41}$$

where

$$M_1 = \frac{2t_1^2\cos\sigma}{[-\ln c]^{\frac{1}{3}}}\left[(\ln(2c\sin\sigma))^2 + \left(\sigma - \frac{\pi}{2}\right)^2\right]^{\frac{1}{6}}\exp\left(\sum_{n=1}^{\infty} a_n\cos n\sigma\right) \tag{4.42}$$

and

$$\begin{aligned} A_1 = \left(\sum_{n=1}^{\infty} a_n\sin n\sigma\right) + 2\tan^{-1}\left(\frac{t_1\sin\sigma}{1+t_1\cos\sigma}\right) \\ -2\tan^{-1}\left(\frac{t_1\sin\sigma}{1-t_1\cos\sigma}\right) + \frac{1}{3}\tan^{-1}\left(\frac{2\sigma-\pi}{2\ln(2c\sin\sigma)}\right) - \sigma \end{aligned} \tag{4.43}$$

We are now in a position to find the coefficients a_n in (4.26) using a method known as collocation. To do so we truncate the infinite series after $N-1$ terms and introduce the N mesh points :-

$$\sigma_M = \frac{\pi(M-\frac{1}{2})}{N} \qquad \text{for} \quad M = 1, 2, \ldots, N \tag{4.44}$$

Substituting our expressions for u and v into (4.39) and evaluating the resulting equation at the N collocation points we obtain N non-linear algebraic equations for the N unknowns $\{a_n\}_{n=1}^{N-1}$ and t_1. This system can now be solved using Newton's method. Due to the symmetry of the model all the odd numbered a_n's should be zero. This provides a reassuring check that the iterative method has converged to the correct root. Having found the a_n's (4.25) gives us expressions for the components of the velocity at every point in the t plane.

Now by integrating (4.34) and (4.35) the shape of the free boundary can be determined. However to determine the constants of integration we must find the relative position of a point on the free boundary to a point on the fixed boundary. An obvious pair of points to choose are 1 and S since we already know their relative separation in the x direction is 0.5 which means we only have to calculate their vertical separation. To do this we take as our path of integration that shown below from 1 to S through P.

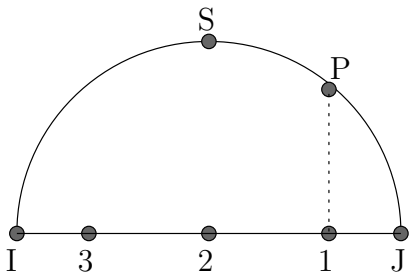


Figure 4.6: Path of integration from 1 to S.

We can already find the change in y from P to S by integrating (4.35) so we only need to construct a means of evaluating the change from 1 to P. By the chain rule :-

$$\frac{dz}{dt} = \frac{dz}{df}\frac{df}{dt} \tag{4.45}$$

$$= \frac{1}{\zeta}\frac{df}{dt} \tag{4.46}$$

$$= \frac{1+t^2}{\pi\zeta t(1-t^2)} \tag{4.47}$$

which on substituting for ζ from (4.25) gives :-

$$\frac{dz}{dt} = -\left(\frac{i}{\pi t_1^2}\right)\left(\frac{1}{t(1-t^2)}\right)\left(\frac{t+t_1}{1+tt_1}\right)\left(\frac{t-t_1}{1-tt_1}\right)\frac{[-\ln c]^{\frac{1}{3}}}{[-\ln c(1-t^2)]^{\frac{1}{3}}}e^{-\Omega(t)} \quad (4.48)$$

On 1P define $t = t_1 + si$ where $s \in [0, (1-t_1^2)^{\frac{1}{2}}]$. Then :-

$$\frac{dz}{dt} = \frac{dz}{ds}\frac{ds}{dt} \quad (4.49)$$

$$= \frac{1}{i}\frac{dz}{ds} \quad (4.50)$$

Thus :-

$$\frac{dz}{ds} = \left(\frac{1}{\pi t_1^2}\right)\left(\frac{1}{t(1-t^2)}\right)\left(\frac{t+t_1}{1+tt_1}\right)\left(\frac{t-t_1}{1-tt_1}\right)\frac{[-\ln c]^{\frac{1}{3}}}{[-\ln c(1-t^2)]^{\frac{1}{3}}}e^{-\Omega(t)} \quad (4.51)$$

On substituting in for t in terms of s and equating imaginary parts we obtain :-

$$\frac{dy}{ds} = M_2 \cos A_2 \quad (4.52)$$

where

$$M_2 = \left(\frac{[-\ln c]^{\frac{1}{3}}}{\pi t_1^2}\right)\left(\frac{s^2(4t_1^2+s^2)}{[(1-t_1^2+s^2)^2+4t_1^2s^2][(1+t_1^2)^2+t_1^2s^2][(1-t_1^2)^2+t_1^2s^2]}\right)^{\frac{1}{2}} \times$$
$$\left(\frac{\exp\left[-\sum_{n=1}^{N-2}2a_n(t_1^2+s^2)^{\frac{n}{2}}\cos\left(n\tan^{-1}\left(\frac{s}{t_1}\right)\right)\right]}{[t_1^2+s^2]\left[(\ln(c((1-t_1^2+s^2)^2+4t_1^2s^2)^{\frac{1}{2}}))^2+\left(\tan^{-1}\left(\frac{2t_1s}{1-t_1^2+s^2}\right)\right)^2\right]^{\frac{1}{3}}}\right)^{\frac{1}{2}} \quad (4.53)$$

and

$$A_2 = \tan^{-1}\left(\frac{2t_1s}{1-t_1^2+s^2}\right) - \tan^{-1}\left(\frac{s}{t_1}\right) - \tan^{-1}\left(\frac{st_1}{1+t_1^2}\right)$$
$$+\tan^{-1}\left(\frac{s}{2t_1}\right) + \frac{1}{3}\tan^{-1}\left(\frac{\tan^{-1}\left(\frac{2t_1s}{1-t_1^2+s^2}\right)}{-\ln[c((1-t_1^2+s^2)^2+4t_1^2s^2)^{\frac{1}{2}}]}\right) \quad (4.54)$$
$$+\tan^{-1}\left(\frac{st_1}{1-t_1^2}\right) - \sum_{n=1}^{N-2}a_n(t_1^2+s^2)^{\frac{n}{2}}\sin\left(n\tan^{-1}\left(\frac{s}{t_1}\right)\right) \quad (4.55)$$

Thus integrating this from $s = 0$ to $s = (1-t_1^2)^{\frac{1}{2}}$ gives us the change in y from 1 to P. Using a similar approach to this, it is in principle possible to find the corresponding point in the z plane to every point in the t plane. This would then allow us to produce a plot of the components of the velocity at all points in the real x,y plane whereas

	T [N]	0.0	0.05	0.1
U [m/s]	F	G		
0.5	0.5	0.0	0.002	0.004
0.2	0.2	0.0	0.0125	0.025
0.1	0.1	0.0	0.05	0.1
0.05	0.05	0.0	0.2	0.4

Table 4.1: Parameter values used and how they relate to U and T.

with the present information we could only plot the velocity components as they vary over the t plane (except at the free surface where we have a relationship between the points in the t plane and those in the z plane).

A program which performs all the above calculations is included in Appendix A. The derivatives of u and v with respect to σ have been approximated by finite differences for ease of computation. The program solves the system of non-linear algebraic equations using the NAG library routine C05NBF and performs the integrations numerically using the routine D01AJF. The program was tested to prove that the solutions were independent of the choice of c. The modulus of the a_n's is found to be rapidly decreasing as n increases which should ensure that the truncation of the power series has not caused any significant error. With a choice of 80 collocation points a_{79} is of $O(10^{-3})$.

Graphical representations of results produced by the program, using 80 collocation points, can be seen on pages 28 and 29. The results displayed are in dimensional form (since dimensionless velocity plots are difficult to compare for different U's which can lead to misinterpretations) where the units of distance are centimetres and the units of velocity are centimetres per second. The parameters used and how they relate to the surface tension T and the uniform velocity U (having taken $L = 0.1\text{m}$, $g = 10\text{m/s}^2$ and $\rho = 1000\text{kg/m}^2$) are displayed in table 4.1. For the free surface plots the height of the rim has been taken as $y = 10\text{cm}$ and the free surface has been discontinued down the side of the nozzle before the numerical integration required becomes difficult. Of course the results could have been interpreted differently by choosing a different pair of consistent values for L and U for any pair F and G.

From these results we see how for any given U increasing the surface tension causes the free surface to rise fractionally higher (note the surface tension of water is about 0.07N and that the addition of a surfactant will cause a reduction of the surface

tension). This rise only becomes comparable with the no surface tension rising height when the flow rate is made very small. The increase in the rising height becomes more significant if we reduce the flow rate even further than those of the results shown or increase the size of T far beyond the parameter ranges in which we are interested. The increase in surface tension can also be seen to cause a reduction in the horizontal surface velocity, u. Thus the effect of a lowered surface tension is to increase the maximum horizontal velocity and reduce the maximum rising height producing a flatter surface. As would be expected the reduction of U causes a decrease in the rising height and the gap between the free surface and the rim.

The results for zero surface tension produced here are in good agreement with similar results (using only 60 collocation points) shown in [5]. In [5] they note that in the case of a small F the shape of the free surface is very closely approximated by that of a pouring flow. A pouring flow consists of an infinite reservoir of fluid held back behind a vertical barrier. As the free surface extends away from the barrier it tends to some undisturbed constant height. Since this undisturbed height is greater than the height of the barrier the fluid pours over the top of the barrier and down the side remaining in contact at all times. It differs from our nozzle problem in the fact that the fluid extends away from the barrier to infinity where it is at rest. In particular for $F < 0.21$ the free surface shape of the pouring flow exactly matches that of the nozzle flow for $x > 0$ (for further details on pouring flows see [10]).

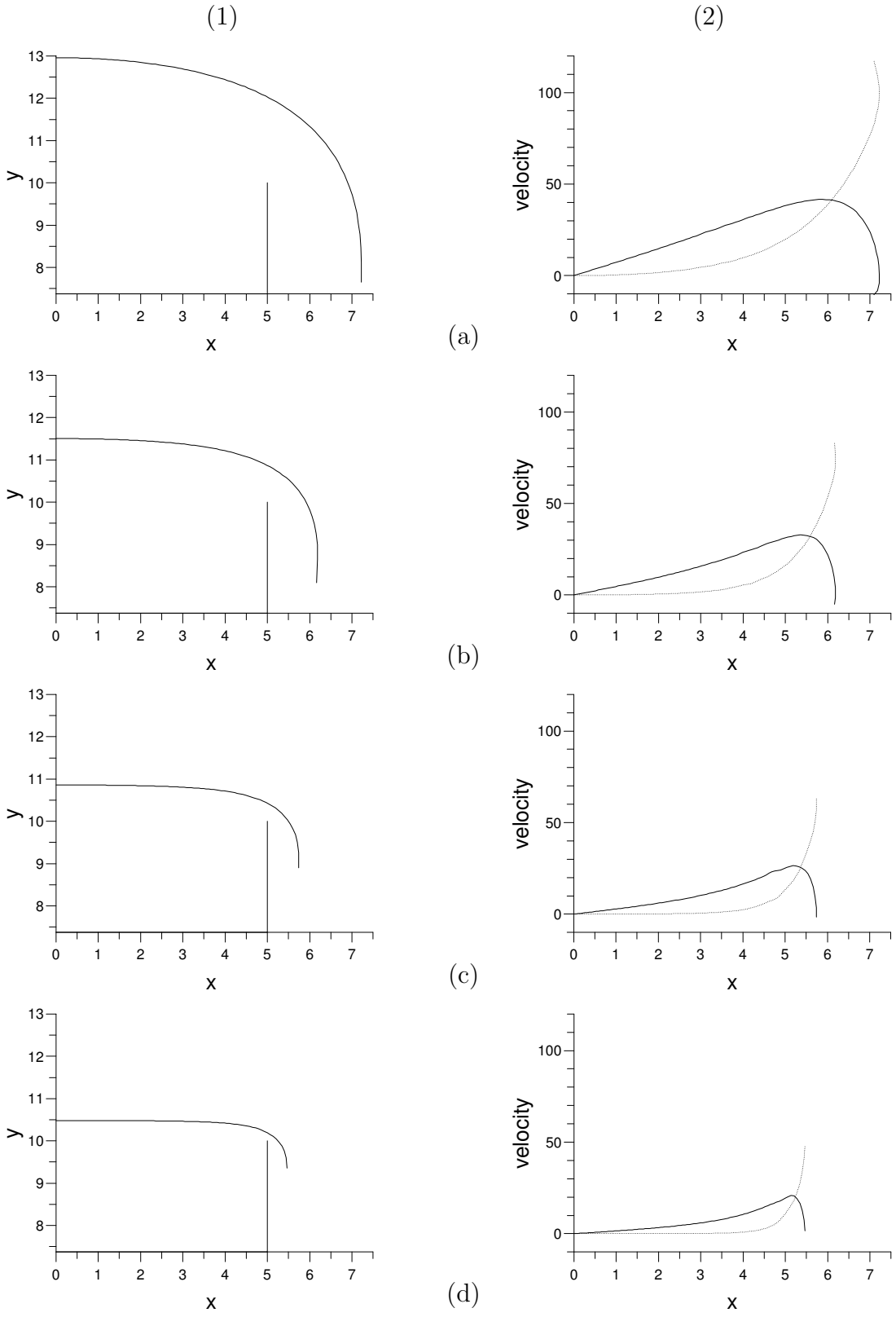


Figure 4.7: (1) The free surface shape, and (2) the surface velocity components (solid line for u and dotted line for $-v$) for $T = 0.05$ and a) $U = 0.5$, b) $U = 0.2$, c) $U = 0.1$ and d) $U = 0.05$.

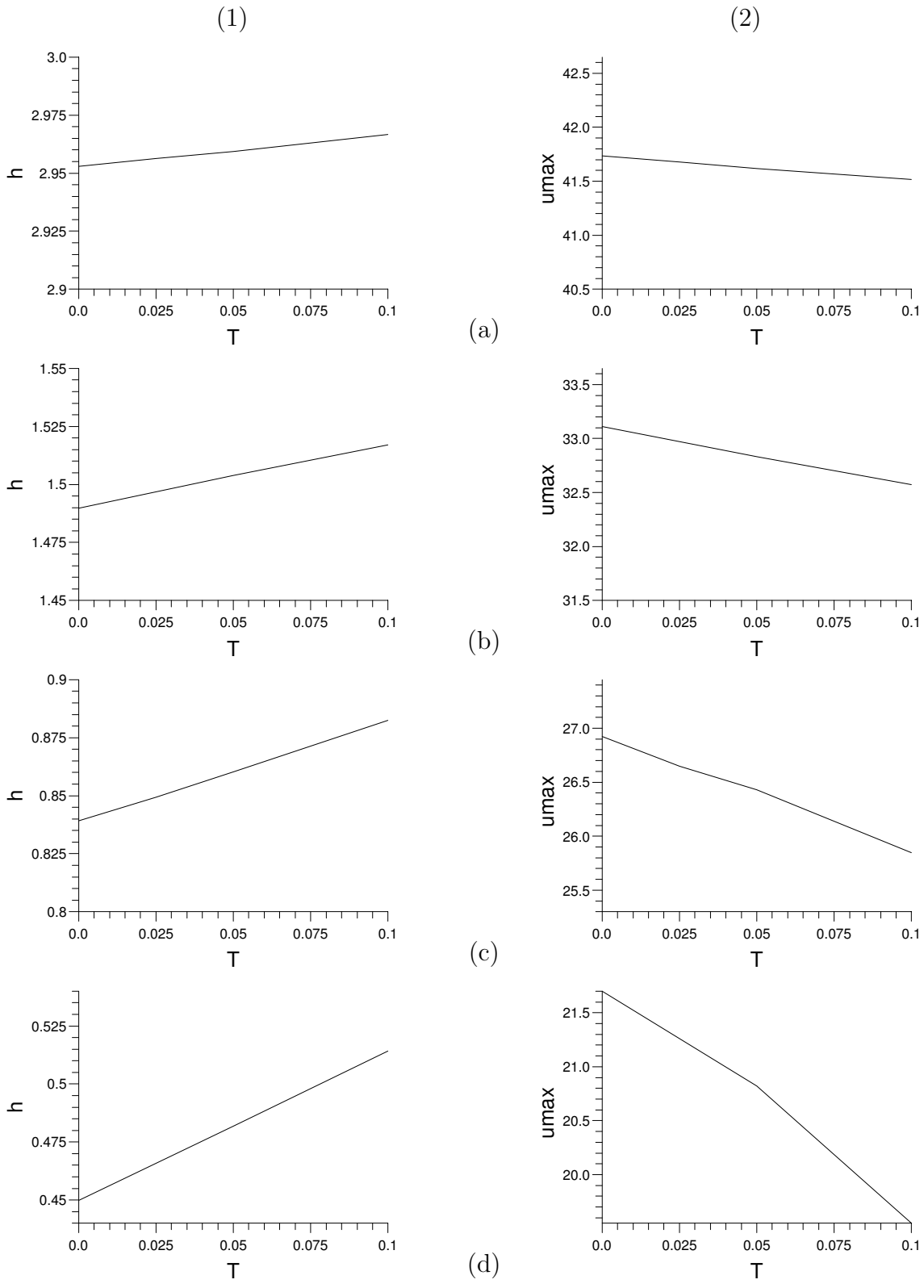


Figure 4.8: (1) Plots of h, the maximum rising height, and (2) plots of umax, the maximum horizontal surface velocity, against T for a) $U = 0.5$, b) $U = 0.2$, c) $U = 0.1$ and d) $U = 0.05$.

Chapter 5

A 3-Dimensional Model

In three dimensions we assume that the flow is axisymmetric. Thus a suitable diagram of the problem is shown below in figure 5.1.

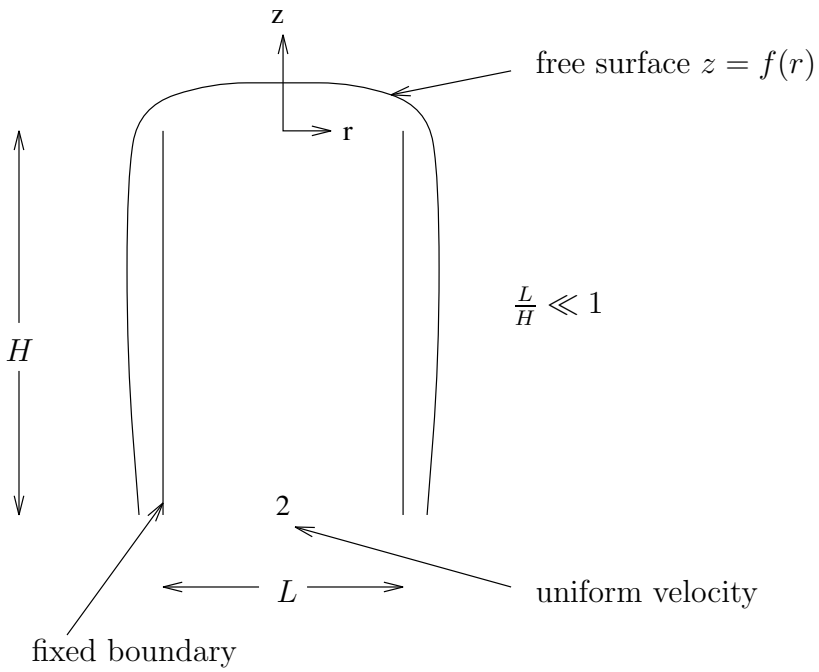


Figure 5.1: A cross-sectional diagram of the axisymmetric 3-dimensional model.

As in the 2-dimensional case we assume the flow is steady, incompressible, irrotational and inviscid as well as being uniform at 2.

5.1 Dimensional Model

Deriving a model in the same manner as in chapter 2 leads to the following set of dimensional equations :-

$$\begin{aligned}
\nabla^2\phi &= 0 \qquad \text{in fluid} && (5.1)\\
\phi_r &= 0 \qquad \text{on } \; r = \frac{1}{2}L \;,\; -H < z < 0 && (5.2)\\
\phi_z &= \phi_r f' \qquad \text{on } \; z = f(r) && (5.3)\\
\frac{1}{2}|\nabla\phi|^2 - \frac{T\kappa}{\rho} + gz &= C \qquad \text{on } \; z = f(r) && (5.4)\\
\phi_r &= 0 \qquad \text{on } \; z = -H \;,\; r \leq \frac{1}{2}L && (5.5)\\
\phi_z &= U \qquad \text{on } \; z = -H \;,\; r \leq \frac{1}{2}L && (5.6)\\
\phi_r &= 0 \qquad \text{on } \; z = -K \;,\; \frac{1}{2}L \leq r \leq R && (5.7)\\
\phi_z &= -\frac{UL^2}{|4R^2 - L^2|} \quad \text{on } \; z = -K \;,\; \frac{1}{2}L \leq r \leq R && (5.8)
\end{aligned}$$

where

$$\begin{aligned}
\nabla^2 &= \frac{\partial^2}{\partial r^2} + \frac{1}{r}\frac{\partial}{\partial r} + \frac{\partial^2}{\partial z^2} && (5.9)\\
\kappa &= \frac{f''}{(1+f'^2)^{\frac{3}{2}}} + \frac{f'}{r(1+f'^2)^{\frac{1}{2}}} && (5.10)\\
R &= f^{-1}(-K) && (5.11)
\end{aligned}$$

5.2 Non-Dimensionalisation

Once again taking U and L as typical velocity and length scales a suitable non-dimensionalisation is :-

$$\mathbf{u} = U\tilde{\mathbf{u}} \quad , \quad \mathbf{r} = L\tilde{\mathbf{r}} \quad , \quad f = L\tilde{f} \quad , \quad \phi = UL\tilde{\phi} \quad , \quad R = L\tilde{R}$$

which on substituting into the above model and dropping the tildes gives the following set of non-dimensional equations.

$$\begin{aligned}
\nabla^2\phi &= 0 \qquad \text{in fluid} && (5.12)\\
\phi_r &= 0 \qquad \text{on } \; r = \frac{1}{2} \;,\; -M_1 < z < 0 && (5.13)\\
\phi_z &= \phi_r f' \qquad \text{on } \; z = f(r) && (5.14)
\end{aligned}$$

$$\frac{1}{2}|\nabla\phi|^2 + \frac{z}{F^2} - G\kappa = C \qquad \text{on} \quad z = f(r) \tag{5.15}$$

$$\phi_r = 0 \qquad \text{on} \quad z = -M_1 \ , \ r \leq \frac{1}{2} \tag{5.16}$$

$$\phi_z = 1 \qquad \text{on} \quad z = -M_1 \ , \ r \leq \frac{1}{2} \tag{5.17}$$

$$\phi_r = 0 \qquad \text{on} \quad z = -M_2 \ , \ \frac{1}{2} \leq r \leq R \tag{5.18}$$

$$\phi_z = -\frac{1}{|4R^2 - 1|} \quad \text{on} \quad z = -M_2 \ , \ \frac{1}{2} \leq r \leq R \tag{5.19}$$

5.3 An Asymptotic Solution

As in chapter 2 consideration of (5.15), assuming ϕ_r, ϕ_z, f' and f'' are $O(1)$, shows that $f = F^2 C \ll 1$, and thus to $O(1)$, $f = 0$. We shall again model the rim of the cylinder like a sink. Such a circular sink can be built up from a continuous distribution of 3-dimensional sinks. After some analysis we find :-

$$\phi \sim \frac{1}{4\pi}\int_0^{2\pi} \frac{1}{(r^2 + z^2 - r\cos\alpha + \frac{1}{4})^{\frac{1}{2}}} d\alpha \qquad \text{near} \quad r = \frac{1}{2} \ , \ z = 0 \tag{5.20}$$

Thus to $O(1)$ the non-dimensional model has become :-

$$\nabla^2\phi = 0 \qquad \text{in fluid} \tag{5.21}$$

$$\phi_r = 0 \qquad \text{on} \quad r = \frac{1}{2} \ , \ -M_1 < z < 0 \tag{5.22}$$

$$\phi_z = 0 \qquad \text{on} \quad r \leq \frac{1}{2} \ , \ z = 0 \tag{5.23}$$

$$\phi_r = 0 \qquad \text{on} \quad z = -M_1 \ , \ r \leq \frac{1}{2} \tag{5.24}$$

$$\phi_z = 1 \qquad \text{on} \quad z = -M_1 \ , \ r \leq \frac{1}{2} \tag{5.25}$$

$$\phi \sim \frac{1}{4\pi}\int_0^{2\pi} \frac{1}{(r^2 + z^2 - r\cos\alpha + \frac{1}{4})^{\frac{1}{2}}} d\alpha \qquad \text{near rim} \tag{5.26}$$

However, unlike in the 2-dimensional case there does not exist an easily derived analytical solution. Therefore we shall resort to a numerical solution. The singularity of condition (5.26) would create difficulties in a numerical approach to a solution for ϕ. However, if we reformulate the problem in terms of a stream function this is easily overcome.

For a 3-dimensional axisymmetric flow we define the stream function ψ by :-

$$u = -\frac{1}{r}\frac{\partial\psi}{\partial z} \tag{5.27}$$

$$v = \frac{1}{r}\frac{\partial \psi}{\partial r} \tag{5.28}$$

where u and v are the components of the velocity in the r and z directions respectively. This satisfies the requirement that $(\mathbf{u}.\nabla)\psi = 0$ so that ψ is constant along streamlines.

Since the flow is uniform at $z = -M_1$ this implies $\psi = \frac{1}{2}r^2$ on $z = -M_1$. Now the axis and free boundary form one streamline and the fixed boundary forms another. Hence :-

$$\psi = \frac{1}{8} \quad \text{on} \quad r = \frac{1}{2} \ , \ -M_1 < z < 0 \tag{5.29}$$

$$\psi = 0 \quad \text{on} \quad r = 0 \ , \ -M_1 < z < 0 \tag{5.30}$$

$$\psi = 0 \quad \text{on} \quad z = 0 \ , \ r < \frac{1}{2} \tag{5.31}$$

$$\psi = \frac{1}{2}r^2 \quad \text{on} \quad z = -M_1 \ , \ r \leq \frac{1}{2} \tag{5.32}$$

From this we see how the condition that ϕ is singular at $z = 0$, $r = \frac{1}{2}$ has become the more managable condition of a jump in ψ.

We now have a complete set of boundary conditions but we still require an equation satisfied by ψ in the fluid. Recalling the fact that $\mathbf{u}$ satisfied $\nabla \times \mathbf{u} = 0$ we have :-

$$\frac{1}{r}\begin{vmatrix} \mathbf{e}_r & r\mathbf{e}_\theta & \mathbf{e}_z \\ \frac{\partial}{\partial r} & \frac{\partial}{\partial \theta} & \frac{\partial}{\partial z} \\ -\frac{1}{r}\frac{\partial \psi}{\partial z} & 0 & \frac{1}{r}\frac{\partial \psi}{\partial r} \end{vmatrix} = 0 \tag{5.33}$$

$$\Rightarrow \quad -\mathbf{e}_\theta \left[\frac{\partial}{\partial r}\left(\frac{1}{r}\frac{\partial \psi}{\partial r} \right) + \frac{1}{r}\frac{\partial^2 \psi}{\partial z^2} \right] = 0 \tag{5.34}$$

$$\Rightarrow \quad r\left(\frac{\partial^2 \psi}{\partial r^2} + \frac{\partial^2 \psi}{\partial z^2} \right) - \frac{\partial \psi}{\partial r} = 0 \tag{5.35}$$

Approximating this with a finite difference scheme gives :-

$$\psi_{i,j} = \frac{1}{4}\left[\left(1 - \frac{1}{2i} \right)\psi_{i+1,j} + \left(1 + \frac{1}{2i} \right)\psi_{i-1,j} + \psi_{i,j+1} + \psi_{i,j-1} \right] \tag{5.36}$$

where $\psi_{i,j} = \psi(ih, -jh)$, h being the mesh size.

Discretizing the boundary conditions we therefore have :-

$$\psi_{I,j} = \frac{1}{8} \quad \text{for} \quad 0 < j \leq J \tag{5.37}$$

$$\psi_{0,j} = 0 \quad \text{for} \quad 0 \leq j \leq J \tag{5.38}$$

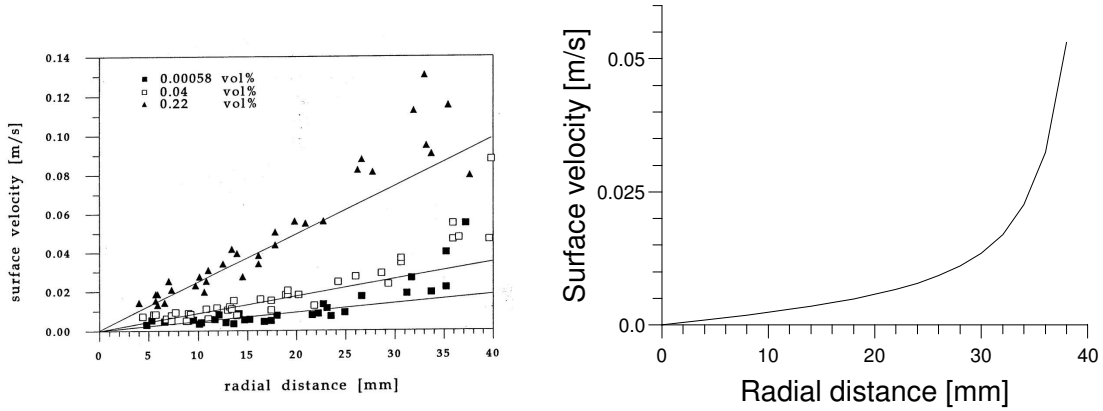
$$\psi_{i,0} = 0 \quad \text{for} \quad 0 \leq i < I \tag{5.39}$$

$$\psi_{i,J} = \frac{1}{2}(ih)^2 \quad \text{for} \quad 0 \leq i \leq I \tag{5.40}$$

where I and J are the maximum values that i and j can take.

This system was solved using the Jacobi iterative method producing the results shown on page 35. Comparing these with those from the 2-dimensional model (see page 16) we see that the effect of the rim although not quite as far reaching is basically the same. Again our assumption that the velocity remains $O(1)$ not surprisingly fails near the rim.

Figure 5.2 below shows the radial component of the surface velocity, u, as it varies with r, as predicted by the above solution and as measured experimentally by Grunnet-Jepsen. The experimental results for 0.00058 vol% of teepol are the same as those of pure water. The relevant parameter values are $L = 8$cm and $U = 1.0445$cm/s. From these results we can see that away from the rim the asymptotic solution gives a good estimate for u in the case of pure water.



Experimental results Numerical solution

Figure 5.2: A comparison of experimental results with the numerical solution.

As in the 2-dimensional case the above approximation breaks down as the sink is approached when the appropriate length scales are much smaller and the velocity scales much larger than was initially assumed. Thus we need to consider an inner problem near $r = \frac{1}{2}L$, $z = 0$.

At this point ideally we might like to proceed in a similar manner to that of chapter 4 to produce a complete numerical solution to the entire flow rather than proceeding with matching the outer and inner solutions. However, in axisymmetric flow the complex potential $\phi + i\psi$ cannot be written as the function of one complex variable which is a function of r and z. Therefore to produce a complete numerical

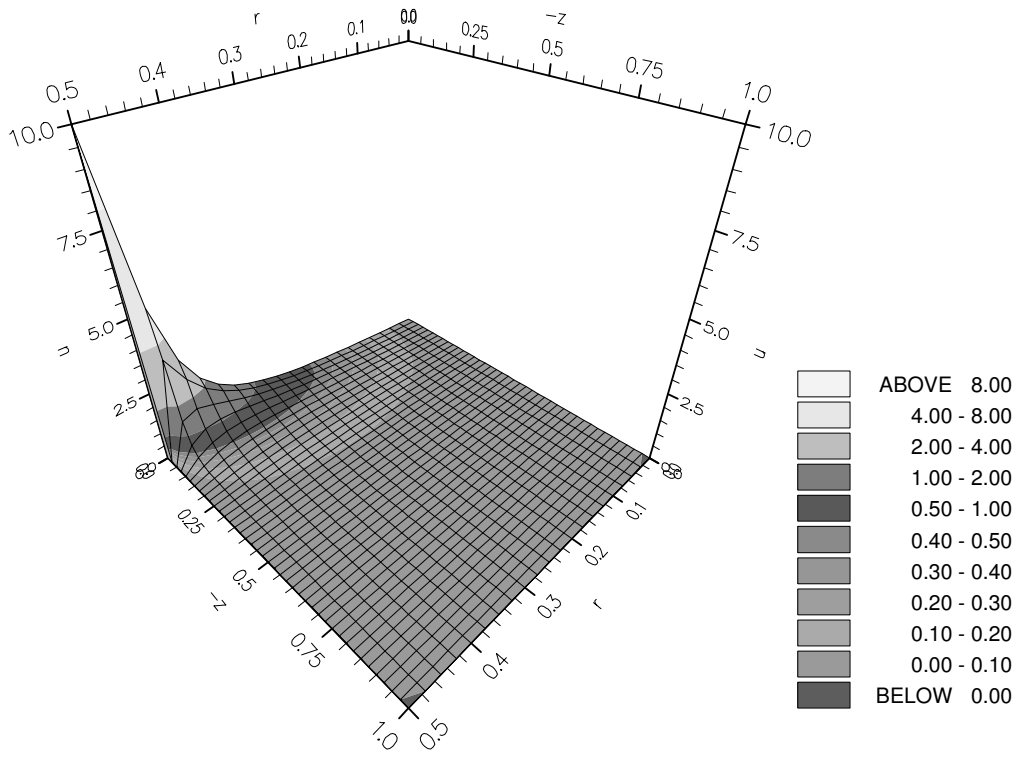


Figure 5.3: Graph of the outer solution for u.

solution in this case we would have to work in the unknown physical domain of the flow and solve the system of equations defined in section 5.2 . This would involve the use of a finite element approximation on a grid which is initial constructed in some estimated domain and then reconstructed as the iterative process causes the position of the free boundary to move until eventually some convergence criterion is satisfied.

Thus in this case it is much better to proceed by considering the inner problem near the rim in order that it can be matched with the above outer solution. In the 2-dimensional case rescaling the equations near the rim does not produce any obviously small terms which could be neglected to simplify the problem, which was why we resorted to a numerical approach. However, in the case of the 3-dimensional axisymmetric flow if we look more closely at the behaviour of the equations near the rim by using the change of variables $r = \frac{1}{2} + \delta\hat{r}$, $z = \delta\hat{z}$ and $f = \delta\hat{f}$ then (5.12) becomes :-

$$\frac{\partial^2\phi}{\partial\hat{r}^2} + \frac{\partial^2\phi}{\partial\hat{z}^2} + \frac{2\delta^2}{(1+2\delta\hat{r})}\frac{\partial\phi}{\partial\hat{r}} \quad = \quad 0 \tag{5.41}$$

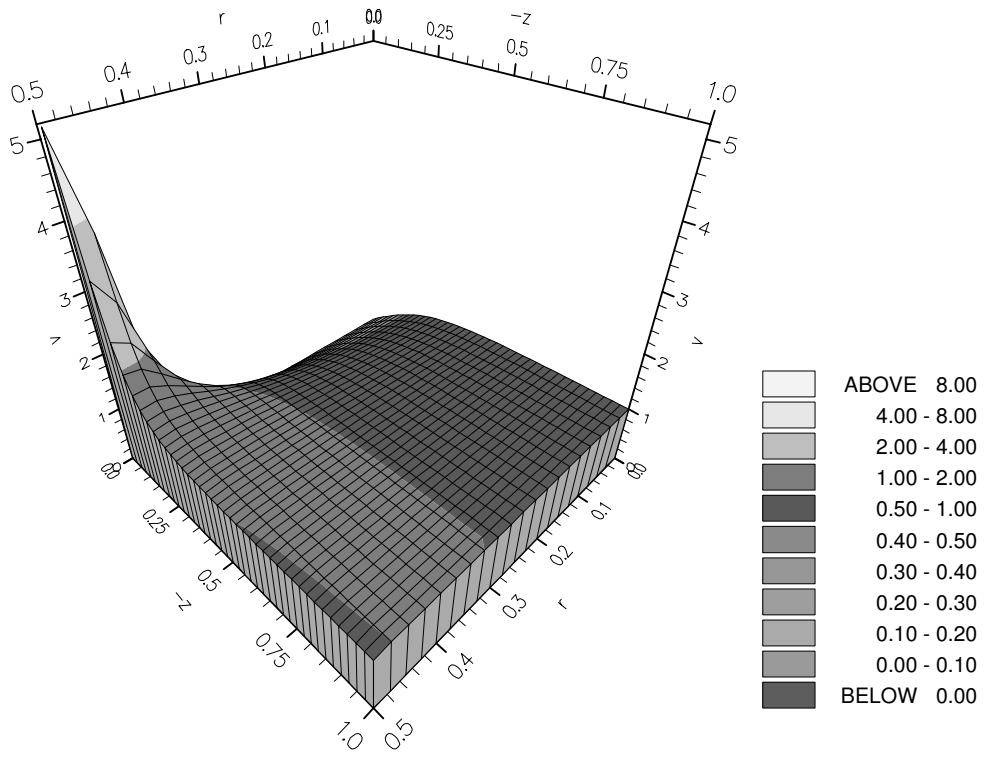


Figure 5.4: Graph of the outer solution for v.

and (5.15) becomes :-

$$\frac{|\nabla\hat{\phi}|^2}{2\delta^2} + \frac{\delta\hat{z}}{F^2} - \frac{G\hat{f}''}{\delta\left(1+\hat{f}'^2\right)^{\frac{3}{2}}} - \frac{2G\hat{f}'}{(1+2\delta\hat{r})\left(1+\hat{f}'^2\right)^{\frac{1}{2}}} \;=\; C \qquad (5.42)$$

In the outer solution the only significant term in Bernoulli's equation was that which came from the inclusion of gravity. However, near the rim both the velocity term and the gravity term are important. Thus we require that $\delta = O(F^{\frac{2}{3}})$. Also the last term in both (5.41) and (5.42) is small in comparison to the other terms in each equation, and hence can be neglected. The loss of these two terms means that the the remaining equations for the flow near the rim are exactly the same as those in the 2-dimensional case. Thus the inner solution is simply that of a 2-dimensional pouring flow and will hence rise to a constant height which when matched with the outer solution will determine the constant C. An important condition to enable the matching of the outer and inner solutions is that they both have the same flux over the rim. A program to determine the inner pouring flow solution numerically could easily be written if more time was available.

Chapter 6

Surface Tension Gradients

As was shown in chapter 2 the existence of surface tension gradients is only possible if the fluid is viscous. In practice the fluids used contain small amounts of surfactant causing them to be slightly viscous and creating the surface tension gradients which are observed experimentally.

Ideally we would like to be able to build this variable surface tension into a model of the flow. However in practice the manner in which the surface tension varies is not known a priori and so must also be determined in the solution.

In [2] they state that their experimental results show that near the centre of the surface the radial velocity, v_r, is proportional to r, and hence the relative surface expansion rate is constant. They proceed to produce a similarity solution for a thin layer of the fluid at the surface. By choosing non-dimensional time and length scales as $\hat{t} = a^{-1}$ and $\hat{l} = \sqrt{\nu a^{-1}}$, where a is unknown and ν is the kinematic viscosity, they define $\eta = z\sqrt{\nu a^{-1}}$. Assuming the stream function ψ can be defined by the pair of equations $v_r = ar\psi'(\eta)$ and $v_z = -2\sqrt{a\nu}\psi$ they solve the Navier-Stokes equations having taken the free surface to be $\eta = 0$. The resulting solution gives :-

$$\frac{dT}{dr} = -ra\rho\sqrt{a\nu}\frac{d^2\psi}{d\eta^2}(0) \tag{6.1}$$

$$\frac{d\ln A}{dt} = \left[-\frac{d^2\psi}{d\eta^2}(0)\frac{r\rho\sqrt{\nu}}{2\sqrt{2}}\right]^{-\frac{2}{3}}\left[\frac{dT}{dr}\right]^{\frac{2}{3}} \tag{6.2}$$

$$\delta = 3\sqrt{\nu}\left(\frac{d\ln A}{dt}\right)^{-\frac{1}{2}} \tag{6.3}$$

where δ is the thickness of the surface layer. Equation (6.1) therefore predicts that $T \propto r^2$. Comparing this to the experimental results they find that the constant of

proportionality predicted by the model is incorrect although it is of the right order. In the case of a pure fluid (6.2) states that the relative surface expansion rate is zero which is clearly incorrect. They, therefore, add to this equation the constant $\left[\frac{d\ln A}{dt}\right]_0$ which is the relative surface expansion rate of the pure fluid. This improves the accuracy of the constant of proportionality in (6.1) but it is still not correct. Finally the third equation is found to predict that this surface layer is typically only a few millimetres thick. One of their conclusions is that the surfactant produces an additional flow field which is superimposed on the basic pure liquid flow.

However, the study of surface chemistry (see for example [8]) shows us that the surface tension is dependent upon the concentration of the surfactant in the flow whereas the above model was based solely on the experimental evidence and nowhere incorporated the dependence of the surface tension on the concentration. Trying to produce an adhoc model based on the experimental results like this is not really a satisfactory approach. Instead we need to consider in more detail how the surface tension is related to the concentration.

One model of this dependence is based upon the Gibbs absorption equation (see [8]) and gives us :-

$$\Gamma = -\frac{1}{R\Theta}\frac{\partial T}{\partial \ln C} \tag{6.4}$$

where

- T is the surface tension,
- Γ is the excess surface concentration of the surfactant,
- C is the concentration of the surfactant in the sub-surface layer and
- R and Θ are constants.

Since the concentrations are small it is assumed that Γ is approximately equal to the surface concentration of the surfactant, C_s. At equilibrium a typical plot of T against $\log C$ is as shown in figure 6.1. This shows that at low concentrations the surface tension is almost equal to that of the pure solvent (e.g. water) but there exist a range of concentration values over which the surface tension drops significantly before once

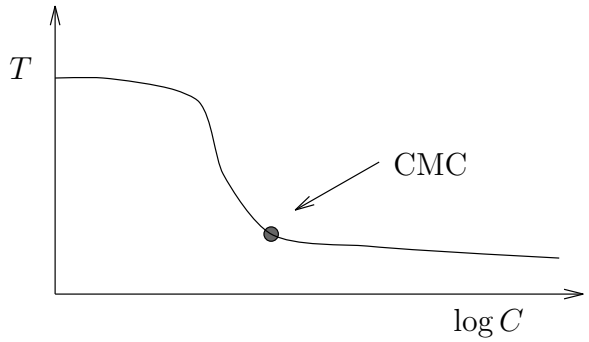


Figure 6.1: A plot of how surface tension varies with concentration.

again levelling off at a lower value. The concentration at which the surface tension ceases to decrease rapidly is known as the critical micelle concentration (CMC).

An alternative model consists of three separate equations independently formulated over the early part of this century by Langmuir, Szyszowski and Franklin. These are :-

$$C_s = \frac{bC}{C+a} \tag{6.5}$$

$$T_0 - T = R\Theta b \ln\left(\frac{C}{a}+1\right) \tag{6.6}$$

$$T_0 - T = -R\Theta b \ln\left(1-\frac{\Gamma}{b}\right) \tag{6.7}$$

respectively, where T_0, a and b are constants. Although independently developed they are consistent in the sense that from any two the third can be derived (assuming $C_s \approx \Gamma$). This second model would appear to be easier to use since each equation only involves two of the three variables T, C_s and C (assuming $C_s \approx \Gamma$).

To incorporate this into a viscous model systematically we would need to model the concentration of the surfactant throughout the flow. Using this model we can then relate the surface tension to the concentration using the above equations.

Chapter 7

Conclusion

We have considered flow through the overflowing cylinder restricting our analysis to the case of an inviscid fluid since the viscosity of the fluids used is very small. This was shown in the production of the model to lead to the implication of a constant surface tension whereas experimentally the surface tension is found to increase fractionally from the centre to the rim. Since this increase is very small (typically of the order 0.001N) taking a constant value would seem a reasonable assumption. Through the detailed numerical solution in the two dimensional case we have been able to produce results which predict that the lowering of the surface tension will give rise to a flatter surface which has a larger horizontal velocity. The model however only predicts small rises in the horizontal velocity whereas experimentally large rises are seen. It would therfore seem likely that, as proposed, the small changes in the surface tension, which mean that there exists a surface tension gradient, are responsible for the marked change. The fact that the surface shapes for the nozzle flow and the pouring flow are the same at low flow rates would suggest that the main effect on the free surface shape comes from near the rim where the surface has a high curvature. The asymptotic solutions in both the three and two dimensional cases show that the main variation to the components of velocity of the fluid occurs near the surface. The comparison of the experimental results with the numerical outer solution showed that in the case of pure water the horizontal component of the surface velocitys are in good agreement.

Further work is needed on a comprehensive viscous model which incorporates a variable surface tension which is determined by the concentration of the surfactant in the fluid near to the surface. Such a model could prove to be an extensive project if it is to convincingly build in the effects of concentration and accurately predict the large rise in the horizontal surface velocity which is observed experimentally.

Appendix A

The Numerical Program

```
c    Collocation  and integration program

       Program God
       implicit none
       integer m,n,lwa,lw,liw
       parameter (n=80,m=101,lwa=(n*(3*n+13))/2,lw=2000,liw=lw/4)
       real*8 a(n),fnorm,tol,fvec(n),wa(lwa),F06EJF,X02AJF,F,G,
     &        pi,gap1,a1,a2,b2,aa,bb,aber,epr,epa,res1,res2,w(lw),
     &        fch,u,v,xco(m),yco(m),uco(m),vco(m)
       integer i,j,iw(liw),ifail,num,fnum,its
       external C05NBF,F06EJF,X02AJF,D01AJF,fcn,fch
       common /count/ num
       common /intnum/ fnum
       common /pars/ F,G,its

       ifail = 1
       epa = 0.0d0
       epr = 1.0d-4
       pi = 4.0d0*atan(1.0d0)
       aa = pi/2.0d0
       F = 0.1d0
       G = 100.0d0
       gap1 = aa/float(m)
       xco(1) = 0.0d0
       yco(1) = 1.0d0
       uco(1) = 0.0d0
       vco(1) = 0.0d0
       tol = sqrt(X02AJF())

c    Set initial estimate for a

       do j = 1,n
          a(j) = 0.1d-3
       enddo

c    Calling NAG library routine to solve n nonlinear equations

       call C05NBF(fcn,n,a,fvec,tol,wa,lwa,ifail)

c    Outputing values of a(n)
```

```
      open(3,file='colloc0.dat')
      open(2,file='colloc00.dat')
      fnorm = F06EJF(n,fvec,1)
      if (ifail.eq.0) then
         write(3,90) tol
         write(3,100) fnorm
         write(3,110)
         write(3,120) a
         write(2,130) a
       else
         write(3,*) ifail,fnorm,tol
         if (ifail.gt.1) write(3,120) a
       endif
       close(2)

c     Using the NAG library to integrate from t1 to S to evaluate yco(1)

       a1 = acos(a(n))
       a2 = 0.0d0
       b2 = sqrt(1.0d0-a(n)*a(n))

       ifail = -1
       fnum = 2
       call D01AJF(fch,a1,aa,epa,epr,res1,aber,w,lw,iw,liw,ifail)

       ifail = -1
       fnum = 3
       call D01AJF(fch,a2,b2,epa,epr,res2,aber,w,lw,iw,liw,ifail)

       yco(1) = yco(1)+res1+res2
       print*,yco(1),res1,res2

c     Using NAG library routine to integrate along the free boundary from S

      do i = 1,m-1
         bb = aa+gap1

         ifail = -1
         fnum = 1
         call D01AJF(fch,aa,bb,epa,epr,res1,aber,w,lw,iw,liw,ifail)

         ifail = -1
         fnum = 2
         call D01AJF(fch,aa,bb,epa,epr,res2,aber,w,lw,iw,liw,ifail)

         uco(i+1) = u(n,a,bb)
         vco(i+1) = v(n,a,bb)
         xco(i+1) = xco(i)+res1
         yco(i+1) = yco(i)+res2
         print*,num,xco(i+1),yco(i+1)
         aa = bb
      enddo

c     Outputing the coordinates of the free boundary

       open(5,file='collocxy.dat')
       write(3,140)
```

```
        write(3,150)(xco(i),yco(i),uco(i),vco(i),i=1,m,4)
        write(5,160)(xco(i),yco(i),uco(i),vco(i),i=1,m)
        write(3,170)its,F,G

        close(5)
        close(3)

   90   format(2x,'tolerance = ',e12.5/)
  100   format(2x,'final 2-norm of the residuals = ',e12.5/)
  110   format(2x,'final approximate solution for the a(n)'/)
  120   format(2x,2f12.5)
  130   format(2x,2f15.8)
  140   format(///,2x,'Coordinates of and velocities at every fourth poi
     &nt on the free boundary',//,5x,'x coordinate',3x,'y coordinate',
     &  4x,'u velocity',5x,'v velocity'/)
  150   format(1x,4f15.8)
  160   format(1x,4e15.5)
  170   format(/2x,'number of iterations used =',i4,//,
     &     2x,'F =',f6.3,//,2x,'G =',f6.3)


        end

c    Subroutines and functions

       subroutine fcn(n,a,fvec,iflag)
       implicit none
       integer iflag,n,k,its
       real*8 fvec(n),a(n),pi,sigk,dsig,u,v,F,G,d2usigk,d2vsigk,usigk
     &,ds,dusigk,vsigk,dvsigk,usigkp,usigkm,vsigkp,vsigkm,t1,t2,t3,t4,t5
       common /pars/ F,G,its

       pi = 4.0d0*atan(1.0d0)

       do k = 1,n
          sigk = pi*(float(k)-0.5d0)/float(n)
          dsig = pi/(4.0d0*float(n))
          ds = 2.0d0*dsig
          usigk = u(n,a,sigk)
          usigkp = u(n,a,sigk+dsig)
          usigkm = u(n,a,sigk-dsig)
          vsigk = v(n,a,sigk)
          vsigkp = v(n,a,sigk+dsig)
          vsigkm = v(n,a,sigk-dsig)
          dusigk = (usigkp-usigkm)/ds
          dvsigk = (vsigkp-vsigkm)/ds
          d2usigk = (usigkp-2.0d0*usigk+usigkm)/(dsig*dsig)
          d2vsigk = (vsigkp-2.0d0*vsigk+vsigkm)/(dsig*dsig)

          t1 = usigk*usigk+vsigk*vsigk
          t2 = usigk*dvsigk-vsigk*dusigk
          t3 = usigk*dusigk+vsigk*dvsigk
          t4 = usigk*d2vsigk-vsigk*d2usigk
          t5 = t4*tan(sigk)/sqrt(t1)-t2*t3*tan(sigk)/(sqrt(t1)*t1)+
     &         t2/(sqrt(t1)*cos(sigk)*cos(sigk))

          print*,sigk,usigk,vsigk
```

```
      fvec(k) = t3-vsigk*cos(sigk)/(F*F*pi*sin(sigk)*t1)+
     &              pi*G*t5*cos(sigk)/abs(cos(sigk))
    enddo

    its = its+1
    print*,its

    return
    end

    function u(n,a,sigk)
    implicit none
    integer n
    real*8 u,sigk,m,an,a(n)

    u = -m(n,a,sigk)*sin(an(n,a,sigk))

    return
    end

    function v(n,a,sigk)
    implicit none
    integer n
    real*8 v,sigk,m,an,a(n)

    v = -m(n,a,sigk)*cos(an(n,a,sigk))

    return
    end

    function m(n,a,sigk)
    implicit none
    integer n,j
    real*8 m,sigk,a(n),c,pi,sum1,m1,m2,m3,m4

    pi = 4.0d0*atan(1.0d0)
    c = 0.2d0
    sum1 = 0.0d0
    do j = 1,n-1
       sum1 = sum1+a(j)*cos(j*sigk)
    enddo
    m1 = 2.0d0*a(n)*a(n)*cos(sigk)
    m2 = exp(log(-log(c))/3.0d0)
    m3 = log(2.0d0*c*sin(sigk))
    m4 = sigk-pi/2.0d0

    m = (m1/m2)*exp(log(m3*m3+m4*m4)/6.0d0)*exp(sum1)

    return
    end

    function an(n,a,sigk)
    implicit none
    integer n,j
    real*8 an,sigk,a(n),c,pi,sum2,an1,an2,an3,an4

    pi = 4.0d0*atan(1.0d0)
```

```
  c = 0.2d0
  sum2 = 0.0d0
  do j = 1,n-1
     sum2 = sum2+a(j)*sin(j*sigk)
  enddo
  an1 = a(n)*sin(sigk)
  an2 = a(n)*cos(sigk)
  an3 = log(2.0d0*c*sin(sigk))
  an4 = sigk-pi/2.0d0

  an = sum2+2.0d0*atan(an1/(1.0d0+an2))-2.0d0*atan(an1/(1.0d0-an2))
&     -sigk+atan(an4/an3)/3.0d0

  return
  end

  function fst(n,a,x)
  implicit none
  integer n,num
  real*8 pi,a(n),x,fst,u,v,ux,vx
  common /count/ num

  num = num+1
  pi = 4.0d0*atan(1.0d0)

  ux = u(n,a,x)
  vx = v(n,a,x)

  fst = -ux*cos(x)/(pi*sin(x)*(ux*ux+vx*vx))

  return
  end

  function gst(n,a,x)
  implicit none
  integer n,num
  real*8 pi,a(n),x,gst,u,v,ux,vx
  common /count/ num

  num = num+1
  pi = 4.0d0*atan(1.0d0)

  ux = u(n,a,x)
  vx = v(n,a,x)

  gst = -vx*cos(x)/(pi*sin(x)*(ux*ux+vx*vx))

  return
  end

  function hst(n,a,x)
  implicit none
  integer n,i
  real*8 c,pi,a(n),x,hst,sum1,sum2,
&        h1,h2,h3,h4,h5,h6,h7,p1,p2,p3,p4,p5,p6,p7,p8

  pi = 4.0d0*atan(1.0d0)
```

```
      c = 0.2d0

      h1 = exp(log(-log(c))/3.0d0)
      h2 = 4.0d0*a(n)*a(n)+x*x
      h3 = a(n)*a(n)+x*x
      p1 = 1.0d0-a(n)*a(n)
      p2 = 1.0d0+a(n)*a(n)
      p3 = a(n)*x
      p4 = p1+x*x
      h4 = p4*p4+4.0d0*p3*p3
      h5 = p2*p2+p3*p3
      h6 = p1*p1+p3*p3
      p5 = -log(c*sqrt(h4))
      p6 = atan(2.0d0*p3/p4)
      h7 = p5*p5+p6*p6
      p7 = atan(x/a(n))
      p8 = 1.0d0
      sum1 = 0.0d0
      sum2 = 0.0d0

      do i = 1,n-1
         p8 = p8*h3
         sum1 = sum1+a(i)*sqrt(p8)*cos(i*p7)
         sum2 = sum2+a(i)*sqrt(p8)*sin(i*p7)
      enddo

      hst = (h1*x/(pi*a(n)*a(n)))*sqrt(h2/(h3*h4*h5*h6))*
     &       exp(-log(h7)/6.0d0)*exp(-sum1)*cos(p6-p7-atan(p3/p2)+
     &       atan(p3/p1)+atan(x/(2.0d0*a(n)))+atan(p6/p5)/3.0d0
     &       -sum2)

      return
      end

      function fch(x)
      implicit none
      integer n,fnum
  310 parameter (n=80)
      real*8 a(n),x,fch,fst,gst,hst
      common /intnum/ fnum

      open(2,file='colloc00.dat')
      read(2,10) a
      close(2)
   10 format(2x,2f15.8)

      if (fnum.eq.1) then
         fch = fst(n,a,x)
      else if(fnum.eq.2) then
         fch = gst(n,a,x)
      else
         fch = hst(n,a,x)
      endif

      return
      end
```

Bibliography

[1] D.J.M. Bergink-Martens, H.J. Bos, A. Prins, and B.C. Schulte. Surface dilation and fluid dynamical behaviour of newtonian liquids in an overflowing cylinder: Part1. *Journal of Colloid and Interface Science*, 138(1):1–9, 1990.

[2] D.J.M. Bergink-Martens, H.J. Bos, A. Prins, and B.C. Schulte. Surface dilation and fluid dynamical behaviour of newtonian liquids in an overflowing cylinder: Part2. *Journal of Colloid and Interface Science*, 165(1):221–228, 1994.

[3] G. Birkhoff and D. Carter. Rising plane bubbles. *Journal of Mathematics and Mechanics*, 6:769–779, 1957.

[4] R.C. Darton, H. Grunnet-Jepsen, P.D. Thomas, and P.B. Whalley. Foam stability and structure in absorption and distillation, 1994. Presented to AIChE Annual Meeting, San Francisco.

[5] F. Dias and J.M. Vanden-Broeck. Flows emerging from a nozzle and falling under gravity. *Journal of Fluid Mechanics*, 213:465–477, 1990.

[6] L.D. Landau and E.M. Lifshitz. *Fluid Mechanics*, page 23. Pergamon Press, second edition, 1987.

[7] H. Lewy. A note on harmonic functions and a hydrodynamical application. *Proceedings of the American Mathematical Society*, 3:111–113, 1952.

[8] M.J. Rosen. *Surfactant and Interfacial Phenomena*, pages 65–84. A Wiley Interscience Publication, second edition, 1989.

[9] R.M.S.M. Schulkes. The evolution of capillary fountains. *Journal of Fluid Mechanics*, 261:223–252, 1994.

[10] J.M. Vanden-Broeck and J.B. Keller. Pouring flows. *The Physics of Fluids*, 29:3958–3961, December 1986.